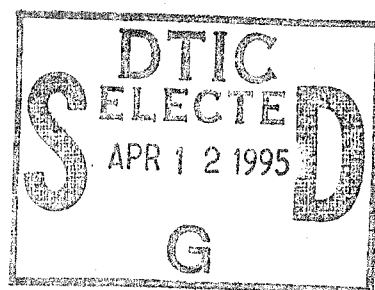


**Technical Report
1008**

Physical Optics Polarization Scattering Matrix for a Right-Angle Dihedral



J.G. Verly

7 February 1995

Lincoln Laboratory
MASSACHUSETTS INSTITUTE OF TECHNOLOGY
LEXINGTON, MASSACHUSETTS



Prepared for the Department of the Air Force under
Contract F19628-95-C-0002.

Approved for public release; distribution is unlimited.

19950410 077

DTIC QUALITY INSPECTED 8


This report is based on studies performed at Lincoln Laboratory, a center for research operated by Massachusetts Institute of Technology. The work was sponsored by the Department of the Air Force under Contract F19628-95-C-0002.

This report may be reproduced to satisfy needs of U.S. Government agencies.

The ESC Public Affairs Office has reviewed this report, and it is releasable to the National Technical Information Service, where it will be available to the general public, including foreign nationals.

This technical report has been reviewed and is approved for publication.

FOR THE COMMANDER


Gary Tutungian
Administrative Contracting Officer
Contracted Support Management

Non-Lincoln Recipients

PLEASE DO NOT RETURN

Permission is given to destroy this document
when it is no longer needed.

MASSACHUSETTS INSTITUTE OF TECHNOLOGY
LINCOLN LABORATORY

PHYSICAL OPTICS POLARIZATION SCATTERING
MATRIX FOR A RIGHT-ANGLE DIHEDRAL

J.G. VERLY
Group 21

TECHNICAL REPORT 1008

7 FEBRUARY 1995

Accession For	
NTIS CRA&I	<input checked="checked" type="checkbox"/>
DTIC TAB	<input type="checkbox"/>
Unannounced	<input type="checkbox"/>
Justification	
By	
Distribution /	
Availability Codes	
Dist	Avail and/or Special
A-1	

Approved for public release; distribution is unlimited.

LEXINGTON

MASSACHUSETTS

ABSTRACT

Using the geometrical optics (GO) and physical optics (PO) approximations, a correct, complete, ready-to-use formula is derived for the backscatter (monostatic) polarization scattering matrix (PSM) of the perfectly conducting right dihedral at arbitrary incidence angle. The absence of such a result from the literature is surprising given that the dihedral's PSM is needed in many applications, such as in the calibration of polarimetric radars, including synthetic aperture radars (SAR), in the generation of simulated polarimetric radar imagery, and in automatic target recognition (ATR). Because the new results provided are important to many researchers who may not be experts in electromagnetic theory (as is often the case for the computer-vision researchers working on ATR), the report is relatively self-contained and takes the reader from the definitions of PSMs and complex radar cross-sections, through the mathematical formulation of Huygen's Principle, the combined use of GO and PO, and changes of polarization bases, to the derivation, discussion, and simplification of the dihedral's PSM.

TABLE OF CONTENTS

Abstract	iii
List of Illustrations	vii
1. INTRODUCTION	1
2. BACKGROUND	5
2.1 Fields	5
2.2 Scattering	5
2.3 Polarization Scattering Matrix	7
2.4 Complex Radar Cross-Sections	9
2.5 Change of Polarization Basis	10
2.6 Huygen's Principle	12
2.7 Geometrical and Physical Optics Approximations	13
3. BACKSCATTERED E-FIELD FOR DIHEDRAL	15
3.1 Single-Bounce Integral Expression	16
3.2 Double-Bounce Integral Expression	16
3.3 Complete Integral Expression	17
3.4 Simple Expressions for P^{S_1} and P^{S_2}	18
3.5 Simple Expressions for $\bar{Q}_{\hat{p}_t}^{S_1}$ and $\bar{Q}_{\hat{p}_t}^{S_2}$	19
3.6 Structures of the Illuminated Regions S_{12} and S_{21}	19
3.7 Simple Expressions for $P^{S_1 S_2}$ and $P^{S_2 S_1}$	25
3.8 Simple Expressions for $\bar{Q}_{\hat{p}_t}^{S_1 S_2}$ and $\bar{Q}_{\hat{p}_t}^{S_2 S_1}$	27
3.9 Final Expression for the Backscattered Fields	29
3.10 Backscattered Field for \hat{k}_t Orthogonal to Crease	31
4. DISCUSSION OF RELATION BETWEEN n/l AND b/a	33
4.1 Fundamental Observations	33
4.2 Partitioning of the Viewing Sphere	34
4.3 Physical Interpretation	34
4.4 Interpretation of Parameter d_x	35

TABLE OF CONTENTS

(Continued)

5. POLARIZATION SCATTERING MATRIX OF DIHEDRAL	41
5.1 Single-Bounce Complex Radar Cross-Section	41
5.2 Double-Bounce Complex Radar Cross-Section	42
5.3 Relative Importance of Single- and Double-Bounce Complex Radar Cross Sections	43
5.4 Double-Bounce Complex Radar Cross Section on the Symmetry Axis	44
5.5 C-RCS Matrix in Circular Basis	44
APPENDIX A – TRANSFORMATION OF SCATTERING MATRIX UNDER CHANGE OF POLARIZATION BASIS	47
A.1 Transformation of Basis Vectors	47
A.2 Transformation of Fields	47
A.3 Transformation of Scattering Matrices	49
APPENDIX B – ALTERNATE FORMULAS FOR THE TOTAL BACKSCATTERED FIELD	53
REFERENCES	55

LIST OF ILLUSTRATIONS

Figure No.		Page
1	Scattering geometry.	6
2	Dihedral geometry.	15
3	S_1S_2 interaction.	23
4	S_2S_1 interaction.	24
5	Geometry for studying sign of $l_z/l_x - b/a$.	36
6	Partitioning of the viewing sphere according to the sign of $n/l - b/a$ for (a) a long dihedral (large b/a) and (b) a short dihedral (small b/a).	37
7	Interpretation of boundary case $l_z/l_x = b/a$ in term of ray casting.	38
8	Graphical interpretation of parameter d_x .	39

1. INTRODUCTION

The right-angle dihedral (DI) corner reflector is an important reference device for calibrating radar systems. It is often used in conjunction with the right-angle trihedral (TRI) corner reflector, the scattering properties of which are, to some degree, complementary.

1. The strongest returns from a DI are due to double-bounce interactions, in which the incident wave successively hits both faces of the DI before being returned towards the source (thus, DIs are known as *double-bounce* or *even-bounce* scatterers). In contrast, the strongest returns from a TRI are due to triple-bounce interactions, in which the incident wave hits all three faces of the TRI in succession (thus, TRIs are known as *triple-bounce* or *odd-bounce* scatterers).
2. The DI produces a strong return for simultaneous transmit right (or left) circular polarization and receive right (or left) circular polarization. In contrast, the TRI produces a strong return for opposite transmit and receive circular polarizations.
3. The backscatter pattern of the DI is broad in a plane perpendicular to its crease and narrow in planes containing it. In contrast, the backscatter pattern of the TRI is relatively narrow.

Even though these properties, as well as others, are well documented, the literature does not readily provide formulas for the backscatter (or monostatic) polarization scattering matrix (PSM) of elementary scatterers (such as the dihedral and trihedral) at arbitrary incidence angles.

The absence of such formulas may result from the fact that fully polarimetric radars are relatively new. The recent availability of fully polarimetric SAR imagery (e.g., from the ERIM [1], JPL [2], and MIT [3] airborne sensors) has led to a resurgence of interest in polarimetry and to a quest for analytical formulas describing the monostatic PSMs of elementary scatterers at arbitrary incidence angles.

Accurate PSM formulas for elementary scatterers are needed by a class of computer codes predicting the appearance (or signature) of complex targets in polarimetric range profiles or range/cross-range images. For example, SarTool [4] first decomposes CAD models of complex targets into their constituent elementary scatterers and then essentially add their properly transformed PSMs to produce the PSM of the targets. In the case of range profiles and range/cross-range images, the calculation is repeated for each point in the profile or image.

Simple, closed-form expressions for the PSMs of elementary scatterers are also needed by computer-vision/image-understanding researchers developing automatic target recognition (ATR) algorithms. In one line of research, bright, contrasted, point-like features are extracted and labeled, e.g., as being "dihedral-like". Generally, these labels are found using techniques based on the early work of Huynen [5] (e.g., see Cameron and Leung [6]). However, much work remains to be done to solve this difficult "inverse problem."

A number of techniques can be used to predict the PSMs of elementary scatterers, but combining geometrical optics (GO) [7, p. 869] and physical optics (PO) [7, p. 870] provides the simplest possible formulas still having a reasonable degree of accuracy. In the case of the dihedral and trihedral, the author is not aware of any report providing, by one method or another, ready-to-use, accurate, closed-form PSM formulas at arbitrary incidence angle. Blejer [8, 9] comes close to providing such formulas, but the results he gives should be questioned because of likely errors and omissions in the paper by Corona et al. [10] from which these results are derived.

The first goal of the present report is to correct the above problems for the dihedral, thereby providing an accurate set of formulas for the dihedral's monostatic PSM resulting from combined GO and PO. The second goal is to make the report accessible to researchers who need such formulas and are not experts in electromagnetic (EM) theory, as is often the case in the ATR and computer-vision communities.

Now, a brief chronological review of relevant, prior work on the analysis of the dihedral's PSM is provided.

Knott [11] considers an obtuse-angle dihedral, with illumination perpendicular to the crease and with arbitrary polarization. Single-bounce (SB) and double-bounce (DB) returns are handled by using PO to deal with scattering by the last surface encountered (in the SB and DB cases) and GO to deal with reflections from the first surface in the DB case. The goal of the paper is to study the effect of the dihedral angle on radar cross section.

Corona et al. [10] extend Knott's work to arbitrary incidence. Even though their results are correct in the case of normal incidence, they are believed to be erroneous and incomplete in the general case.

Blejer [8, 9] used Corona's incorrect and incomplete results to derive the PSMs of the dihedral and trihedral. These formulas are apparently used in the prediction code SarTool [4].

Griesser et al. [12] consider a problem similar to Knott's (incidence normal to crease; vertical and horizontal polarizations), but they deal with arbitrary dihedral angles, as well as with single-, double-, and triple-bounces, single refractions, and reflection-diffractions, using various combinations of GO, PO, and PTD (physical theory of diffraction).

Corona et al. [13] use a generalization of PO to study the effect of surface loading in the case of orthogonal incidence.

Anderson [14] considers vertical and horizontal polarizations at arbitrary incidence angles on dihedrals with angles no smaller than 60 deg, and uses PO to compute single-, double-, and triple-bounce terms. However, the integrated forms of key surface integrals are not given in the paper.

Atkins and Shin [15] propose a new approach for dealing with multiple bounces between two possibly-disjoint polygonal plates (a special case of which is the dihedral), where they avoid using GO for dealing with intermediate reflections.

This report explores in detail the derivation of the PSM of the (unloaded) right dihedral under the approximations of GO and PO. As already indicated, it is written to make the information accessible to the nonexpert, in particular to researchers in computer-vision and ATR. Thus, this report begins with a brief review of fundamental concepts, such as PSMs, complex radar cross sections, changes of polarization basis, GO, and PO. Then, a general expression for the field backscattered by the dihedral is derived, avoiding the premature combination of SB and DB terms. An important dichotomy arising in the integration of a DB surface integral is carefully considered. Finally, the PSM of the dihedral is derived, the relative contributions of the SB and DB terms are compared, and simplified formulas are derived, which agree with the expression used almost exclusively by those working the inverse problem (e.g., Huynen [5] and Cameron and Leung [6]).

2. BACKGROUND

2.1 Fields

Consider time-harmonic, i.e., monochromatic, EM fields with angular frequency $\omega = 2\pi c/\lambda$, where c is the speed of light and λ the wavelength of interest. Using a time-dependence $e^{j\omega t}$, the electric field at any point \bar{r}_P can be written as [16, p. 46]

$$\bar{E}(\bar{r}_P, t) = \mathcal{R}e\{\bar{E}(\bar{r}_P) e^{j\omega t}\}. \quad (1)$$

This report focuses on the complex, time-independent field $\bar{E}(\bar{r}_P)$, also known as a phasor. The physical field can be retrieved at any time through Equation (1). These remarks also apply to the magnetic field \bar{H} .

In the classical treatment of scattering, the wave incident on the scatterer is assumed to be a plane wave and the scattered wave is an outgoing spherical wave that, in the far zone of the scatterer, can be treated locally as a plane wave.

Plane wave are characterized by their propagation, or wave, vector $\bar{k} = k\hat{k}$, where $k = 2\pi/\lambda$ and, in general, \hat{x} denotes the unit vector corresponding to \bar{x} . In the case of linear polarization characterized by a polarization \hat{p} orthogonal to the propagation direction \hat{k} , the complex field $\bar{E}(\bar{r}_P) \equiv \bar{E}_{\hat{p}}(\bar{r}_P)$ is [16, p. 54]

$$\bar{E}_{\hat{p}}(\bar{r}_P) = E_{\hat{p}} e^{-i\bar{k} \cdot \bar{r}_P} \hat{p} \quad (2)$$

where $E_{\hat{p}}$ is the complex magnitude of the field at $\bar{r}_P = 0$. The case of arbitrary polarization is considered below.

2.2 Scattering

Consider the scattering geometry of Figure 1. The scatterer is assumed to be located near the origin 0 of the (x, y, z) coordinate system, and the sensor is assumed to be located at a point S with spherical coordinates (r, θ, ϕ) . With each S , one associates a unique coordinate system defined by the unit vectors \hat{r} , $\hat{\theta}$, and $\hat{\phi}$: \hat{r} is defined by the vector $\overline{OS} \equiv \bar{r}$; $\hat{\phi}$ is perpendicular to the plane defined by S and the z -axis, and oriented in the sense of increasing ϕ ; and $\hat{\theta}$ is perpendicular to the plane $(\hat{r}, \hat{\phi})$ and oriented in the sense of increasing θ , with the result that the frame $(\hat{r}, \hat{\theta}, \hat{\phi})$ is right-handed. Of course, the sensor position is given by $\bar{r} = r\hat{r}$.

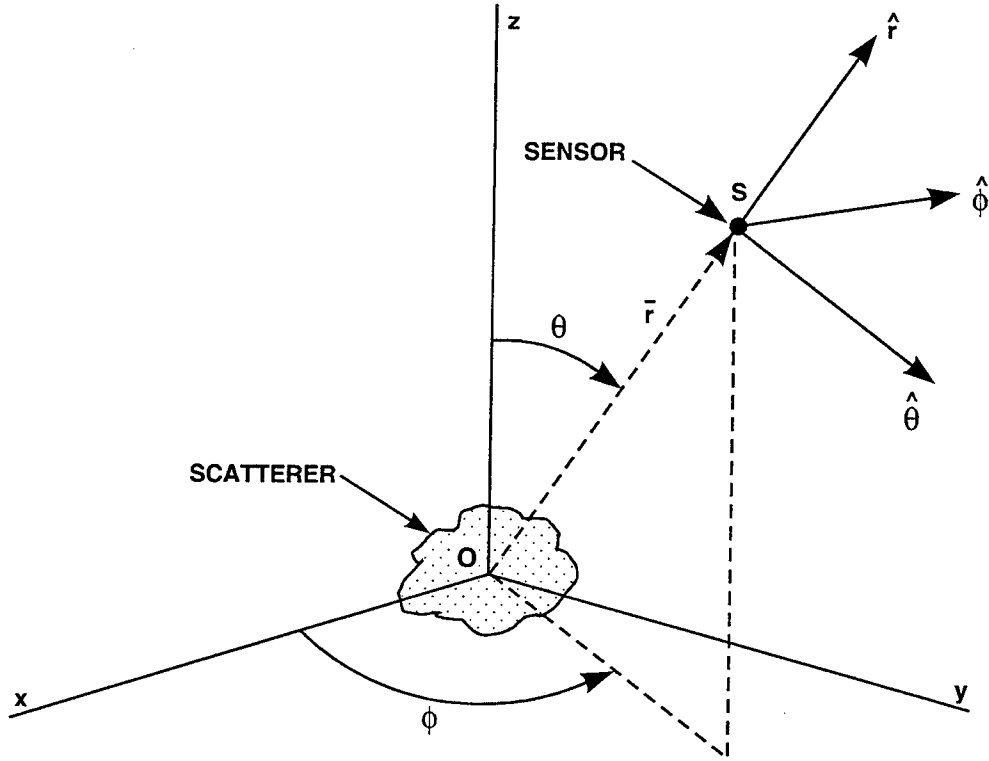


Figure 1. Scattering geometry.

Consider an EM field transmitted from S towards O . If the scatterer is in the far zone of the transmitting antenna, this field can be treated as a plane wave traveling in the $\hat{k} = \hat{k}_t = -\hat{r}$ direction. In the case of linear polarization along \hat{p} (perpendicular to \hat{r}), the "transmitted" complex field $\bar{E}^t(\bar{r}_P)$ can be written as in Equation (2). In the case of arbitrary polarization, $\bar{E}^t(\bar{r}_P)$ can be described in terms of its components in a polarization basis (AB) characterized by its basis vectors \hat{h}_A and \hat{h}_B . A particularly convenient basis for the intended analysis is the (HV) basis (H = horizontal, V = vertical), the basis vectors of which are the vectors $\hat{\phi}$ and $\hat{\theta}$ of Figure 1, i.e., $\hat{h}_H = \hat{\phi}$ and $\hat{h}_V = \hat{\theta}$. Other choices of basis are discussed later. In the (HV) basis, one has

$$\bar{E}^t(\bar{r}_P) = \bar{E}_{\hat{\phi}}^t(\bar{r}_P) + \bar{E}_{\hat{\theta}}^t(\bar{r}_P) \quad (3)$$

with [see Equation (2)]

$$\bar{E}_{\hat{p}_t}^t(\bar{r}_P) = E_{\hat{p}_t}^t e^{-i\bar{k}_t \cdot \bar{r}_P} \hat{p}_t \quad (4)$$

where \hat{p}_t is either $\hat{\phi}$ or $\hat{\theta}$. Equation (3) can thus be written as

$$\bar{E}^t(\bar{r}_P) = \bar{E}^t e^{-i\bar{k}_t \cdot \bar{r}_P} \quad (5)$$

with

$$\bar{E}^t = E_{\hat{\phi}}^t \hat{\phi} + E_{\hat{\theta}}^t \hat{\theta}. \quad (6)$$

The magnitudes and phases of the complex numbers $E_{\hat{\phi}}^t$ and $E_{\hat{\theta}}^t$ fully determine the polarization characteristics of the transmitted field $\bar{E}^t(\bar{r}_P)$. Note that the plane wave described by $\bar{E}^t(\bar{r}_P)$ is a local approximation to a spherical wave originating from S , so that $E_{\hat{\phi}}^t$ and $E_{\hat{\theta}}^t$ should include the $1/r$ attenuation associated with the distance r from S to O . However, this report treats $\bar{E}^t(\bar{r}_P)$ as a true plane wave and, thus, $E_{\hat{\phi}}^t$ and $E_{\hat{\theta}}^t$ as (complex) constants.

The currents induced on the surface of the scatterer by the incoming wave produce a scattered EM field. In the far zone of the scatterer, this field is effectively a spherical wave originating from O that can be approximated locally by a plane wave. Limiting the analysis to the backscattering case (i.e., to transmit and receive sensors co-located at S), the “received” E -field can be expressed as

$$\bar{E}^r(\bar{r}) = E_{\hat{\phi}}^r(\bar{r}) \hat{\phi} + E_{\hat{\theta}}^r(\bar{r}) \hat{\theta}. \quad (7)$$

Note the use of \bar{r} (instead of \bar{r}_P) since one is only interested in the fields at the receiver. Also note that the \bar{r} -dependencies have not been factored out [in contrast to what was done in Equations (5) and (6) with regard to \bar{r}_P].

2.3 Polarization Scattering Matrix

It is well-known [17, 18, 19] that the complex components $E_{\hat{\phi}}^r(\bar{r})$ and $E_{\hat{\theta}}^r(\bar{r})$ of the received field $\bar{E}^r(\bar{r})$ are *linearly* related to the complex components $E_{\hat{\phi}}^t$ and $E_{\hat{\theta}}^t$ characterizing the value of the transmitted field at the origin 0, i.e., of $\bar{E}^t(\bar{r}_P = 0)$. This linear relation is written as

$$\begin{pmatrix} E_{\hat{\phi}}^r(\bar{r}) \\ E_{\hat{\theta}}^r(\bar{r}) \end{pmatrix} = \alpha(k, r) \begin{pmatrix} S_{\hat{\phi}\hat{\phi}} & S_{\hat{\phi}\hat{\theta}} \\ S_{\hat{\theta}\hat{\phi}} & S_{\hat{\theta}\hat{\theta}} \end{pmatrix} \begin{pmatrix} E_{\hat{\phi}}^t \\ E_{\hat{\theta}}^t \end{pmatrix} \quad (8)$$

or

$$\bar{E}^r(\bar{r}) = \alpha(k, r) S \bar{E}^t \quad (9)$$

where the use of the scale factor $\alpha(k, r)$ reflects the lack of universal agreement on the definition of the (polarization) scattering matrix S . Typical values for $\alpha(k, r)$ are

$$1, \frac{e^{-ikr}}{r}, \frac{e^{-ikr}}{kr}. \quad (10)$$

Note the slight, inconsequential abuse of notation for \bar{E}^t and $\bar{E}^r(\bar{r})$. Indeed, these symbols denote 3-D vectors [in the $(\hat{x}, \hat{y}, \hat{z})$ frame] in Equations (6) and (7), and 2-D vectors [in the $(\hat{\phi}, \hat{\theta})$ frame] in Equation 9.

In practice, the elements $S_{\hat{p}_r \hat{p}_t}$ of S (with \hat{p}_r and \hat{p}_t taking either of the values $\hat{\phi}$ or $\hat{\theta}$) can be found as follows. Consider a transmitted field that is linearly polarized along $\hat{p}_t = \hat{\phi}$ or $\hat{p}_t = \hat{\theta}$ and has some arbitrary complex magnitude E_0 . Such a field can be described by Equation (4) with $E_{\hat{p}_t}^t = E_0$. From Equation (6), it follows that

$$\bar{E}^t = E_0 \hat{p}_t. \quad (11)$$

Using this expression in conjunction with Equations (8) and (9), one finds

$$E_{\hat{p}_r}^r(\bar{r}) = \alpha(k, r) S_{\hat{p}_r \hat{p}_t} E_0 \quad (12)$$

so that

$$S_{\hat{p}_r \hat{p}_t} = \frac{1}{\alpha(k, r)} \frac{E_{\hat{p}_r}^r(\bar{r})}{E_0}. \quad (13)$$

Because $E_{\hat{p}_r}^r$ is the component along \hat{p}_r of the field $\bar{E}_{\hat{p}_t}(\bar{r})$ received when the transmitted field has complex amplitude E_0 and polarization \hat{p}_t , one can rewrite (for future use) Equation (13) as

$$S_{\hat{p}_r \hat{p}_t} = \frac{1}{\alpha(k, r)} \frac{\bar{E}_{\hat{p}_t}(\bar{r}) \cdot \hat{p}_r}{E_0}. \quad (14)$$

2.4 Complex Radar Cross-Sections

Because of the lack of agreement on the definition of $\alpha(k, r)$, it is useful to first find the scatterer's complex radar cross sections (C-RCS) $\sqrt{\sigma_{\hat{p}_r \hat{p}_t}}$ for the various combinations of \hat{p}_t and \hat{p}_r , and then express each $S_{\hat{p}_r \hat{p}_t}$ in terms of the corresponding $\sqrt{\sigma_{\hat{p}_r \hat{p}_t}}$ (note that $\sqrt{\sigma_{\hat{p}_r \hat{p}_t}}$ is the symbol denoting each C-RCS). The more familiar radar cross sections (RCS) $\sigma_{\hat{p}_r \hat{p}_t}$ are obtained by taking the square of the magnitude of $\sqrt{\sigma_{\hat{p}_r \hat{p}_t}}$.

The agreed-upon definition for the C-RCS is [8]

$$\sqrt{\sigma_{\hat{p}_r \hat{p}_t}} = \lim_{r \rightarrow \infty} 2\sqrt{\pi} r \frac{\bar{E}_{\hat{p}_t}(\bar{r}) \cdot \hat{p}_r}{E_0} e^{ikr}. \quad (15)$$

In all cases of interest here, the limit in Equation (15) can be ignored, so that the desired relationship is

$$S_{\hat{p}_r \hat{p}_t} = \beta(k, r) \sqrt{\sigma_{\hat{p}_r \hat{p}_t}} \quad (16)$$

where

$$\beta(k, r) = \frac{e^{-ikr}}{2\sqrt{\pi} r \alpha(k, r)}. \quad (17)$$

The values of $\beta(k, r)$ for the three common choices in Equation (10) are

$$\frac{e^{-ikr}}{2\sqrt{\pi} r}, \frac{1}{2\sqrt{\pi}}, \frac{k}{2\sqrt{\pi}}. \quad (18)$$

Equation (15) can be used to define a C-RCS matrix $\sqrt{\sigma}$ analogous to the scattering matrix S in Equations (8) and (9), i.e.,

$$\sqrt{\sigma} = \begin{pmatrix} \sqrt{\sigma_{\hat{\phi}\hat{\phi}}} & \sqrt{\sigma_{\hat{\phi}\hat{\theta}}} \\ \sqrt{\sigma_{\hat{\theta}\hat{\phi}}} & \sqrt{\sigma_{\hat{\theta}\hat{\theta}}} \end{pmatrix}. \quad (19)$$

Clearly

$$S = \beta(k, r)\sqrt{\sigma}. \quad (20)$$

2.5 Change of Polarization Basis

The previously-selected basis vectors $\hat{h}_H = \hat{\phi}$ and $\hat{h}_V = \hat{\theta}$ of the linear basis (HV) are true 3-D space vectors with real-valued components. However, in general, the basis vectors \hat{h}_A and \hat{h}_B defining a basis (AB) may be three-component vectors with complex-valued components. A typical example is the left-right circular basis (LR) with basis vectors \hat{h}_L and \hat{h}_R related to \hat{h}_H and \hat{h}_V by

$$\begin{pmatrix} \hat{h}_L \\ \hat{h}_R \end{pmatrix} = \frac{1}{\sqrt{2}} \begin{pmatrix} 1 & j \\ 1 & -j \end{pmatrix} \begin{pmatrix} \hat{h}_H \\ \hat{h}_V \end{pmatrix} \quad (21)$$

or, symbolically,

$$\hat{h}_{(LR)} = T_{(HV \rightarrow LR)} \hat{h}_{(HV)} \quad (22)$$

where

$$T_{(HV \rightarrow LR)} = \frac{1}{\sqrt{2}} \begin{pmatrix} 1 & j \\ 1 & -j \end{pmatrix} \quad (23)$$

and, in general, $\hat{h}_{(AB)}$ is a “vector,” the elements of which are the unit vectors \hat{h}_A and \hat{h}_B associated with the basis (AB) . In the general case of two bases (AB) and $(A'B')$, one writes

$$\hat{h}_{(A'B')} = T_{(AB \rightarrow A'B')} \hat{h}_{(AB)}. \quad (24)$$

Although the transformation $T_{(HV \rightarrow LR)}$ given in Equation (23) appears to be the one most often used to relate (HV) and (LR) , this transformation is not universally agreed upon [20, p. 17], [8, p. 4].

The effect of a “change of basis” on the scattering matrix is a delicate subject treated in detail in Appendix A, where it is shown that a dual change of basis is actually used, with one change for the transmitted field, and one separate, related change for the received field. If the scattering matrix is given by $S_{(AB)}$ when the transmitted field \bar{E}^t is expressed in basis (AB) , then Equation (A.1) and (A.2) show that the scattering matrix $S_{(A'B')}$ corresponding to \bar{E}^t expressed in basis $(A'B')$ is

$$S_{(A'B')} = U^T S_{(AB)} U \quad (25)$$

with

$$U = T^T \quad (26)$$

where, in general, A^T denotes the transpose of A . Obviously, Equation (25) can also be written as

$$S_{(A'B')} = T S_{(AB)} T^T. \quad (27)$$

Carefully note that one has not said in which basis the received field \bar{E}^r is expressed and that Equation (25) *cannot* generally be derived from Equation (8) by performing a true change of basis (these points are discussed in Appendix A).

For calculation purposes, observe that U and T are both unitary matrices [see Equations (A.9) and (A.10)]. Finally, for future reference, note that the relation between the linear-basis scattering matrix

$$S_{(HV)} = \begin{pmatrix} S_{HH} & S_{HV} \\ S_{HV} & S_{VV} \end{pmatrix} \quad (28)$$

and the corresponding circular-basis scattering matrix

$$S_{(LR)} = \begin{pmatrix} S_{LL} & S_{LR} \\ S_{LR} & S_{RR} \end{pmatrix} \quad (29)$$

is given by

$$S_{(LR)} = \frac{1}{2} \begin{pmatrix} 1 & j \\ 1 & -j \end{pmatrix} \begin{pmatrix} S_{HH} & S_{HV} \\ S_{HV} & S_{VV} \end{pmatrix} \begin{pmatrix} 1 & 1 \\ j & -j \end{pmatrix} \quad (30)$$

or

$$S_{(LR)} = \begin{pmatrix} \frac{S_{HH}-S_{VV}}{2} + j S_{HV} & \frac{S_{HH}+S_{VV}}{2} \\ \frac{S_{HH}+S_{VV}}{2} & \frac{S_{HH}-S_{VV}}{2} - j S_{HV} \end{pmatrix}. \quad (31)$$

Clearly, a similar formula can be written for the C-RCS matrix $\sqrt{\sigma}$.

2.6 Huygen's Principle

The key formula for computing the field $\bar{E}_{\hat{p}_t}$ appearing in Equations (14) and (15) is the mathematical expression of Huygen's principle [16, p. 399, but with $e^{j\omega t}$], i.e.,

$$\bar{E}_{\hat{p}_t}(\bar{r}) = -\frac{ik\omega\mu e^{-ikr}}{4\pi r} [I - \hat{r}\hat{r}] \int_{S'} \bar{J}_{S,\hat{p}_t}(\bar{r}') e^{i\bar{k}\cdot\bar{r}'} dS' \quad (32)$$

where μ is the permeability of the medium (assumed isotropic), S' the surface of the scatterer (with points \bar{r}'), and $\bar{J}_{S,\hat{p}_t}(\bar{r}')$ the surface current induced on S' by a transmitted wave with polarization \hat{p}_t .

The dyadic operator $[I - \hat{r}\hat{r}]$ applied to some arbitrary vector \bar{a} should be interpreted as

$$[I - \hat{r}\hat{r}]\bar{a} = \bar{a} - \hat{r}(\hat{r}\cdot\bar{a}) \quad (33)$$

which has the effect of removing the component of \bar{a} along \hat{r} , thereby yielding the projection of \bar{a} in the plane $(\hat{\theta}, \hat{\phi})$, i.e.,

$$[I - \hat{r}\hat{r}]\bar{a} = \hat{\phi}(\hat{\phi}\cdot\bar{a}) + \hat{\theta}(\hat{\theta}\cdot\bar{a}). \quad (34)$$

The dyadic operator can thus be rewritten as

$$I - \hat{r}\hat{r} = \hat{\phi}\hat{\phi} + \hat{\theta}\hat{\theta}. \quad (35)$$

Note that $e^{-ikr}[I - \hat{r}\hat{r}]$ is a mathematical expression of the fact that $\bar{E}_{\hat{p}_t}(\bar{r})$ is an outgoing spherical wave, which is precisely the assumption made previously in the discussion leading to the definition of the scattering matrix S . In fact, Equation (32) can be used to obtain explicit expressions for the $\hat{\phi}$ and $\hat{\theta}$ components of $\bar{E}_{\hat{p}_t}(\bar{r})$ that appear in Equation (7), but this is not further explored here.

2.7 Geometrical and Physical Optics Approximations

One needs to relate the surface current $\bar{J}_{S,\hat{p}_t}(\bar{r}_P)$ to the transmitted, linearly polarized (along \hat{p}_t) wave characterized by [see Equation (4)]

$$\bar{E}_{\hat{p}_t}^t(\bar{r}_P) = E_{\hat{p}_t}^t e^{-i\bar{k}_t \cdot \bar{r}_P} \hat{p}_t = E_{\hat{p}_t}^t e^{ik\hat{r} \cdot \bar{r}_P} \hat{p}_t. \quad (36)$$

For compatibility with Equations (14) and (15), $E_{\hat{p}_t}^t$ is set to E_0 [see Equation (11)], so that Equation (36) becomes

$$\bar{E}_{\hat{p}_t}^t(\bar{r}_P) = E_0 e^{-i\bar{k}_t \cdot \bar{r}_P} \hat{p}_t = E_0 e^{ik\hat{r} \cdot \bar{r}_P} \hat{p}_t. \quad (37)$$

To find $\bar{J}_{S,\hat{p}_t}(\bar{r}_P)$, one also needs the magnetic field $\bar{H}_{\hat{p}_t}^t$ associated with $\bar{E}_{\hat{p}_t}^t$ [16, p. 55], i.e.,

$$\bar{H}_{\hat{p}_t}^t(\bar{r}_P) = \frac{1}{\omega\mu} \bar{k}_t \times \bar{E}_{\hat{p}_t}^t(\bar{r}_P) = -\frac{k}{\omega\mu} E_0 e^{-i\bar{k}_t \cdot \bar{r}_P} \hat{r} \times \hat{p}_t. \quad (38)$$

The counterpart of Equation (37) is thus

$$\bar{H}_{\hat{p}_t}^t(\bar{r}_P) = H_0 e^{-i\bar{k}_t \cdot \bar{r}_P} \hat{a}_t = H_0 e^{ik\hat{r} \cdot \bar{r}_P} \hat{a}_t \quad (39)$$

with the complex value H_0 given by

$$H_0 = \frac{k}{\omega\mu} E_0 \quad (40)$$

and

$$\hat{a}_t = \begin{cases} \hat{\theta} & \text{if } \hat{p}_t = \hat{\phi} \\ -\hat{\phi} & \text{if } \hat{p}_t = \hat{\theta}. \end{cases} \quad (41)$$

For a number of elementary scatterers of interest (e.g., the dihedral considered later in the report), it is necessary to consider not only single-bounce interactions, but also multi-bounce interactions (e.g., double-bounce in the case of the dihedral). Here, one follows the customary practice of using PO to compute the field backscattered by the last surface participating in a particular interaction, and of using GO to handle scattering by intermediate surfaces. The following analysis relies on the assumption that all scattering surfaces are perfect conductors.

First, the magnetic field $\bar{H}_{\hat{p}_t}^i(\bar{r}')$ incident on the last scattering surface (S') is derived from $\bar{H}_{\hat{p}_t}^t(\bar{r}_P)$ and the scatterer's geometry through the laws of GO. Second, one uses the PO approximation to relate the surface current $\bar{J}_{S,\hat{p}_t}(\bar{r}')$ appearing in Equation (32) to $\bar{H}_{\hat{p}_t}^i(\bar{r}')$, i.e., [7, Equation (38)],

$$\bar{J}_{S,\hat{p}_t}(\bar{r}') = \begin{cases} 2 \hat{n}(\bar{r}') \times \bar{H}_{\hat{p}_t}^i(\bar{r}') & \text{on illuminated part of } S' \\ 0 & \text{on shadowed part of } S' \end{cases} \quad (42)$$

where $\hat{n}(\bar{r}')$ is the unit normal to S' at \bar{r}' .

3. BACKSCATTERED E-FIELD FOR DIHEDRAL

In this section, compact, nonintegral expressions are derived for the field $\bar{E}_{\hat{p}_t}(\bar{r})$ [given by Equation (32)] backscattered from a perfectly conducting dihedral sized and positioned as indicated in Figure 2. Recall that the subscript \hat{p}_t indicates that the field corresponds to a transmitted plane wave linearly polarized along \hat{p}_t . This wave is characterized by the E-field of Equation (37) or, equivalently, by the H-field of Equation (39).

209852-1

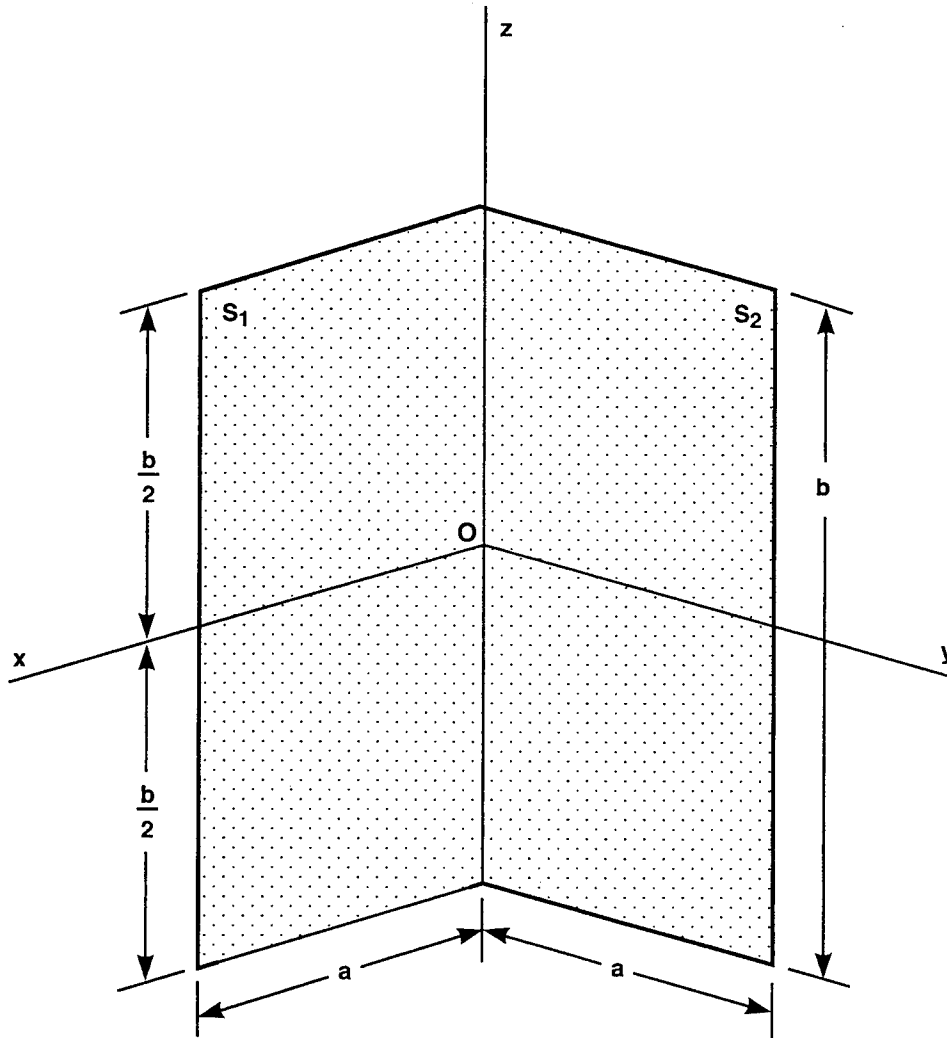


Figure 2. Dihedral geometry.

3.1 Single-Bounce Integral Expression

The dihedral exhibits two distinct single-bounce (SB) interactions. The first corresponds to backscattering of the transmitted wave by the surface S_1 of the side normal to \hat{y} , and the second to backscattering of the same wave by the surface S_2 of the side normal to \hat{x} . Both interactions can be treated jointly by denoting the backscattering surface by S and its normal towards the sensor by \hat{n} .

In the SB case, the field $\bar{H}_{\hat{p}_t}^i$ appearing in Equation (42) is simply given by the transmitted H-field $\bar{H}_{\hat{p}_t}^t$, i.e. [see Equation (39)],

$$\bar{H}_{\hat{p}_t}^i(\bar{r}') = H_0 e^{-i\bar{k}_t \cdot \bar{r}'} \hat{a}_t = H_0 e^{ik\hat{r} \cdot \bar{r}'} \hat{a}_t. \quad (43)$$

Using Equations (32) and (42), one finds that the SB contribution due to S alone is

$$\bar{E}_{\hat{p}_t}^S(\bar{r}) = -\frac{ikE_0 e^{-ikr}}{2\pi r} [I - \hat{r}\hat{r}](\hat{n} \times \hat{a}_t) \int_S e^{2ik\hat{r} \cdot \bar{r}'} dS \quad (44)$$

where \bar{r}' denotes points in S .

3.2 Double-Bounce Integral Expression

The dihedral exhibits two distinct double-bounce (DB) interactions. The first corresponds to backscattering by S_2 of the portion of the transmitted wave that is reflected by S_1 and intercepted by S_2 , and the second is obtained by reversing the roles of S_1 and S_2 . Both interactions can be treated jointly by denoting the reflecting surface (the first) and its normal by S_A and \hat{n}_A , respectively, and the backscattering surface (the second) and its normal by S_B and \hat{n}_B , respectively. The part of S_B illuminated by reflections from S_A is denoted by S_{AB} .

In the DB case, the field $\bar{H}_{\hat{p}_t}^i$ appearing in Equation (42) is obtained by reflecting the transmitted H-field $\bar{H}_{\hat{p}_t}^t$ [given by Equation (39)] essentially according to GO:

1. The wavevector \bar{k}_i is obtained from \bar{k}_t by requiring that the reflection on S_A reverse the sign of the component of \bar{k}_t corresponding to \hat{n}_A (necessarily either \hat{x} or \hat{y}), i.e.,

$$\bar{k}_i = \bar{k}_t - 2(\bar{k}_t \cdot \hat{n}_A)\hat{n}_A. \quad (45)$$

2. The polarization vector \hat{a}_i is obtained from \hat{a}_t by imposing the boundary conditions for the H-field on the perfectly conducting surface S_A , i.e., that (a) the tangential components of the incident and reflected H-fields be equal, and that (b) the sum of their normal components be zero. One finds

$$\hat{a}_i = \hat{a}_t - 2(\hat{a}_t \cdot \hat{n}_A)\hat{n}_A. \quad (46)$$

Therefore,

$$\begin{aligned}\bar{H}_{\hat{p}_t}^i(\bar{r}') &= H_0 e^{-i[\bar{k}_t - 2(\bar{k}_t \cdot \hat{n}_A)\hat{n}_A] \cdot \bar{r}'} [\hat{a}_t - 2(\hat{a}_t \cdot \hat{n}_A)\hat{n}_A] \\ &= H_0 e^{ik[\hat{r} - 2(\hat{r} \cdot \hat{n}_A)\hat{n}_A] \cdot \bar{r}'} [\hat{a}_t - 2(\hat{a}_t \cdot \hat{n}_A)\hat{n}_A].\end{aligned}\quad (47)$$

Again, using Equations (32) and (42), one finds that the DB contribution due to surfaces S_A and S_B encountered in that order is

$$\bar{E}_{\hat{p}_t}^{S_A S_B}(\bar{r}) = -\frac{ikE_0 e^{-ikr}}{2\pi r} [I - \hat{r}\hat{r}] (\hat{n}_B \times [\hat{a}_t - 2(\hat{a}_t \cdot \hat{n}_A)\hat{n}_A]) \int_{S_{AB}} e^{2ik[\hat{r} - (\hat{r} \cdot \hat{n}_A)\hat{n}_A] \cdot \bar{r}'} dS_{AB} \quad (48)$$

where \bar{r}' denotes points in S_{AB} .

3.3 Complete Integral Expression

The Equations (44) and (48) for the SB and DB contributions can be combined to get the total E-field backscattered by the dihedral, i.e., [notice the similarity with Equation (5) in Anderson's paper [14]],

$$\bar{E}_{\hat{p}_t}(\bar{r}) = -\frac{ikE_0 e^{-ikr}}{2\pi r} \left(P^{S_1} \bar{Q}_{\hat{p}_t}^{S_1} + P^{S_2} \bar{Q}_{\hat{p}_t}^{S_2} + P^{S_1 S_2} \bar{Q}_{\hat{p}_t}^{S_1 S_2} + P^{S_2 S_1} \bar{Q}_{\hat{p}_t}^{S_2 S_1} \right) \quad (49)$$

with

$$P^S = (\hat{r} \cdot \hat{n}) \int_S e^{2ik\hat{r} \cdot \bar{r}'} dS \quad (50)$$

$$\bar{Q}_{\hat{p}_t}^S = \frac{[I - \hat{r}\hat{r}](\hat{n} \times \hat{a}_t)}{\hat{r} \cdot \hat{n}} \quad (51)$$

$$P^{S_A S_B} = (\hat{r} \cdot \hat{n}_B) \int_{S_{AB}} e^{2ik[\hat{r} - (\hat{r} \cdot \hat{n}_A)\hat{n}_A] \cdot \bar{r}'} dS_{AB} \quad (52)$$

$$\bar{Q}_{\hat{p}_t}^{S_A S_B} = \frac{[I - \hat{r}\hat{r}](\hat{n}_B \times [\hat{a}_t - 2(\hat{a}_t \cdot \hat{n}_A)\hat{n}_A])}{\hat{r} \cdot \hat{n}_B}. \quad (53)$$

The reason for introducing the apparently superfluous factors $(\hat{r} \cdot \hat{n})$ and $(\hat{r} \cdot \hat{n}_B)$ will become clear later.

In the next sections, one derives compact, closed-form expressions for the four quantities above. To do so, one will express \hat{r} in terms of its components l_x , l_y , and l_z , which are also the direction cosines of the sensor location, i.e.,

$$\hat{r} = (l_x, l_y, l_z) \quad (54)$$

with

$$\begin{cases} l_x &= \sin \theta \cos \phi \\ l_y &= \sin \theta \sin \phi \\ l_z &= \cos \theta. \end{cases} \quad (55)$$

3.4 Simple Expressions for P^{S_1} and P^{S_2}

When $S \equiv S_1$, one has $\hat{n} = \hat{y}$ and $\bar{r}' = (x, 0, z)$, so that Equation (50) becomes

$$\begin{aligned} P^{S_1} &= (\hat{r} \cdot \hat{y}) \int_{S_1} e^{2ik(l_x x + l_z z)} dS_1 \\ &= l_y \left(\int_0^a e^{2ikl_x x} dx \right) \left(\int_{-b/2}^{b/2} e^{2ikl_z z} dz \right). \end{aligned} \quad (56)$$

i.e.,

$$P^{S_1} = abl_y e^{ikal_x} \text{sinc } k'al_x \text{sinc } k'bl_z \quad (57)$$

where

$$\text{sinc } x = \frac{\sin \pi x}{\pi x} \quad (58)$$

and

$$k' = \frac{k}{\pi}. \quad (59)$$

When $S \equiv S_2$, one has $\hat{n} = \hat{x}$ and $\bar{r}' = (0, y, z)$, so that Equation (50) similarly becomes

$$P^{S_2} = abl_x e^{ikal_y} \text{sinc } k'al_y \text{sinc } k'bl_z. \quad (60)$$

3.5 Simple Expressions for $\bar{Q}_{\hat{p}_t}^{S_1}$ and $\bar{Q}_{\hat{p}_t}^{S_2}$

One begins by rewriting the numerator A of the Equation (51) for $\bar{Q}_{\hat{p}_t}^S$ as

$$A = [I - \hat{r}\hat{r}](\hat{n} \times \hat{a}_t) \quad (61)$$

$$= \hat{\theta}(\hat{\theta} \cdot (\hat{n} \times \hat{a}_t)) + \hat{\phi}(\hat{\phi} \cdot (\hat{n} \times \hat{a}_t)) \quad (62)$$

$$= \hat{\theta}(\hat{n} \cdot (\hat{a}_t \times \hat{\theta})) + \hat{\phi}(\hat{n} \cdot (\hat{a}_t \times \hat{\phi})) \quad (63)$$

where one has used Equation (34) and the cyclic property of the mixed product, i.e., $a \cdot (b \times c) = b \cdot (c \times a)$.

1. When $\hat{p}_t = \hat{\phi}$, Equation (41) gives $\hat{a}_t = \hat{\theta}$. Then Equation (61) reduces to $(\hat{n} \cdot \hat{r})\hat{\phi}$, and Equation (51) yields $\bar{Q}_{\hat{\phi}}^S = \hat{\phi}$.
2. When $\hat{p}_t = \hat{\theta}$, Equation (41) gives $\hat{a}_t = -\hat{\phi}$. Then Equation (61) reduces to $(\hat{n} \cdot \hat{r})\hat{\theta}$, and Equation (51) yields $\bar{Q}_{\hat{\theta}}^S = \hat{\theta}$.

As a result

$$\bar{Q}_{\hat{p}_t}^{S_1} = \bar{Q}_{\hat{p}_t}^{S_2} = \hat{p}_t. \quad (64)$$

One motivation for introducing $\hat{r} \cdot \hat{n}$ in Equation (51) was to obtain a unit-length $\bar{Q}_{\hat{p}_t}^{S_1}$.

Equation (64) indicates that the “return” from *each* individual SB interaction is co-polarized with the transmitted wave, both for horizontal transmit ($\hat{\phi}$) and for vertical transmit ($\hat{\theta}$).

3.6 Structures of the Illuminated Regions S_{12} and S_{21}

The problem of determining the region of integration S_{AB} appearing in Equation (52) must be examined carefully, especially because it appears to have been mishandled in the literature.

The region S_{AB} is found by tracing all the rays incident on S_A through their reflections on S_A . Each point of S_B reached (i.e., illuminated) by a ray reflected from S_A is part of S_{AB} . Note that this section is based exclusively on ray tracing, i.e., on techniques from GO.

Each incident ray travels along direction

$$\hat{k}_t = -\hat{r} = (-l_x, -l_y, -l_z) \quad (65)$$

and goes through the plane of S_A at some point \bar{x}_A . If \bar{x}_A is on S_A , then the ray is reflected along direction [see Equation (45) with both sides divided by k]

$$\hat{k}_{AB} = \hat{k}_i = \hat{k}_t - 2(\hat{k}_t \cdot \hat{n}_A)\hat{n}_A \quad (66)$$

and, thus, goes through the plane of S_B at some point \bar{x}_B given by

$$\bar{x}_B = \bar{x}_A + \alpha_{AB} \hat{k}_{AB} \quad (67)$$

where α_{AB} is to be determined.

In specializing these results to the S_1S_2 and S_2S_1 interactions, it is useful to temporarily restrict the analysis to the case

$$\frac{l_y}{l_x} \leq 1, l_z \geq 0. \quad (68)$$

Of course, we are only interested in the case where $l_x, l_y \geq 0$. All these constraints are equivalent to

$$0 \leq \phi \leq \pi/4 \text{ and } 0 \leq \theta \leq \pi/2. \quad (69)$$

These restrictions will be removed later.

3.6.1 S_1S_2 Interaction

Here, one has $\hat{n}_A = \hat{y}$ and thus Equation (66) can yield $\hat{k}_{12} = (-l_x, l_y, -l_z)$. Equation (67) can be written as

$$\begin{pmatrix} 0 \\ y_2 \\ z_2 \end{pmatrix} = \begin{pmatrix} x_1 \\ 0 \\ z_1 \end{pmatrix} + \alpha_{12} \begin{pmatrix} -l_x \\ l_y \\ -l_z \end{pmatrix}. \quad (70)$$

Eliminating α_{12} and solving for (x_1, z_1) , one gets

$$\begin{cases} x_1 &= \frac{l_x}{l_y} y_2 \\ z_1 &= z_2 + \frac{l_z}{l_y} y_2. \end{cases} \quad (71)$$

By imposing the constraint that the intercept point (x_1, z_1) be in S_1 (in order for the incident ray to be reflected), i.e., that

$$0 \leq x_1 \leq a \text{ and } -\frac{b}{2} \leq z_1 \leq \frac{b}{2} \quad (72)$$

one obtains the following constraints on (x_2, z_2)

$$\begin{cases} 0 \leq y_2 \leq a \frac{l_y}{l_x} \\ z_2 + \frac{l_z}{l_y} y_2 + \frac{b}{2} \geq 0 \\ z_2 + \frac{l_z}{l_y} y_2 - \frac{b}{2} \leq 0. \end{cases} \quad (73)$$

In addition, (x_2, z_2) must be in S_2 (in order for the reflected ray to be scattered by S_2), so that

$$\begin{cases} 0 \leq y_2 \leq a \\ -\frac{b}{2} \leq z_2 \leq \frac{b}{2}. \end{cases} \quad (74)$$

These two sets of inequalities fully define S_{12} .

Careful analysis of these constraints reveals that, under the limitations of Equation (68), two canonically different structures for region S_{12} must be considered. The first, S_{12}^+ , corresponds to the case $l_z/l_x \leq b/a$, and the second, S_{12}^- , to $l_z/l_x \geq b/a$ (see Figure 3). This dichotomy appears to have been overlooked in the literature (a more detailed discussion is given later).

3.6.2 S_2S_1 Interaction

Here, one has $\hat{n}_A = \hat{x}$ and thus Equation (66) yields $\hat{k}_{21} = (l_x, -l_y, -l_z)$. Equation (67) can be written as

$$\begin{pmatrix} x_1 \\ 0 \\ z_1 \end{pmatrix} = \begin{pmatrix} 0 \\ y_2 \\ z_2 \end{pmatrix} + \alpha_{21} \begin{pmatrix} l_x \\ -l_y \\ -l_z \end{pmatrix}. \quad (75)$$

Eliminating α_{21} and solving for (y_2, z_2) , one gets

$$\begin{cases} y_2 = \frac{l_y}{l_x} x_1 \\ z_2 = z_1 + \frac{l_z}{l_x} x_1. \end{cases} \quad (76)$$

By imposing the constraint that the intercept point (y_2, z_2) be in S_1 (in order for the incident ray to be reflected), i.e., that

$$0 \leq y_2 \leq a \quad \text{and} \quad -\frac{b}{2} \leq z_2 \leq \frac{b}{2} \quad (77)$$

one obtains the following constraints on (x_1, z_1)

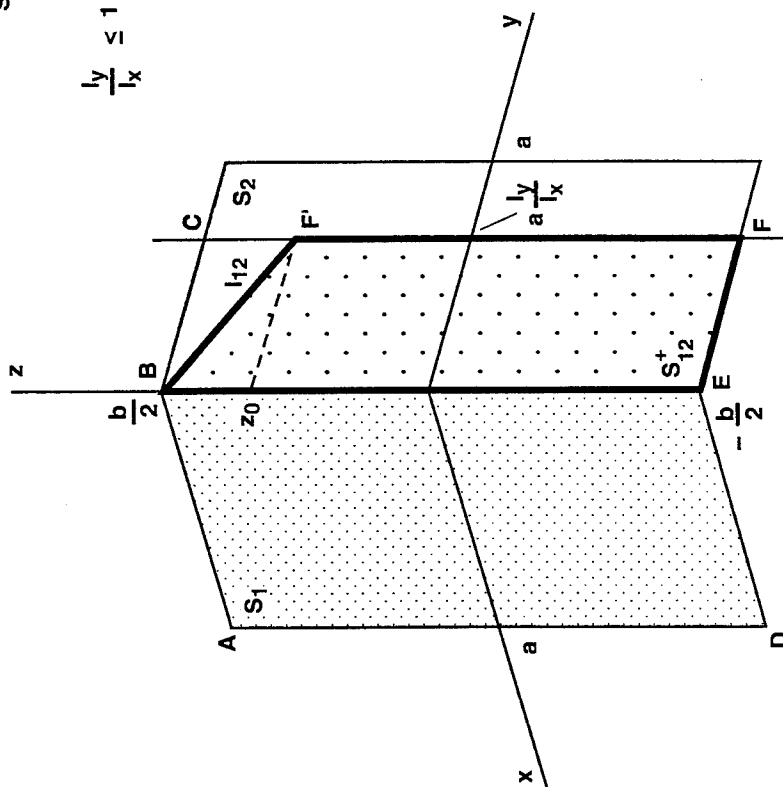
$$\begin{cases} 0 \leq x_1 \leq a \frac{l_x}{l_y} \\ z_1 + \frac{l_z}{l_x} x_1 + \frac{b}{2} \geq 0 \\ z_1 + \frac{l_z}{l_x} x_1 - \frac{b}{2} \leq 0. \end{cases} \quad (78)$$

In addition, (x_1, z_1) must be in S_1 (in order for the reflected ray to be scattered by S_1), so that

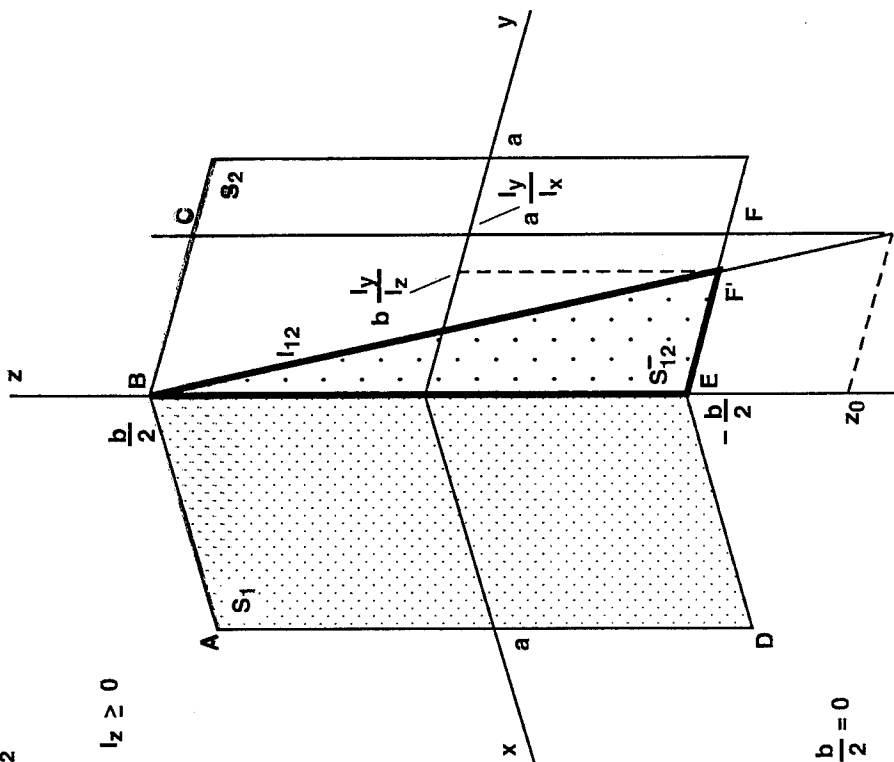
$$\begin{cases} 0 \leq x_1 \leq a \\ -\frac{b}{2} \leq z_1 \leq \frac{b}{2}. \end{cases} \quad (79)$$

These two sets of inequalities fully define S_{21} .

Here also, two canonically different structures for region S_{21} must be considered. The counterpart of Figure 3 is Figure 4.

$S_1 \rightarrow S_2$
 $\frac{l_y}{l_x} \leq 1$ AND $l_z \geq 0$


$$(a) \quad \frac{l_z}{l_x} \leq \frac{b}{a}$$



$$(b) \quad \frac{l_z}{l_x} \geq \frac{b}{a}$$

$$l_{12}: z + \frac{l_z}{l_y} y - \frac{b}{2} = 0$$

$$z_0 = -\frac{b}{2} + a \left(\frac{b}{a} - \frac{l_z}{l_x} \right)$$

Figure 3. $S_1 S_2$ interaction.

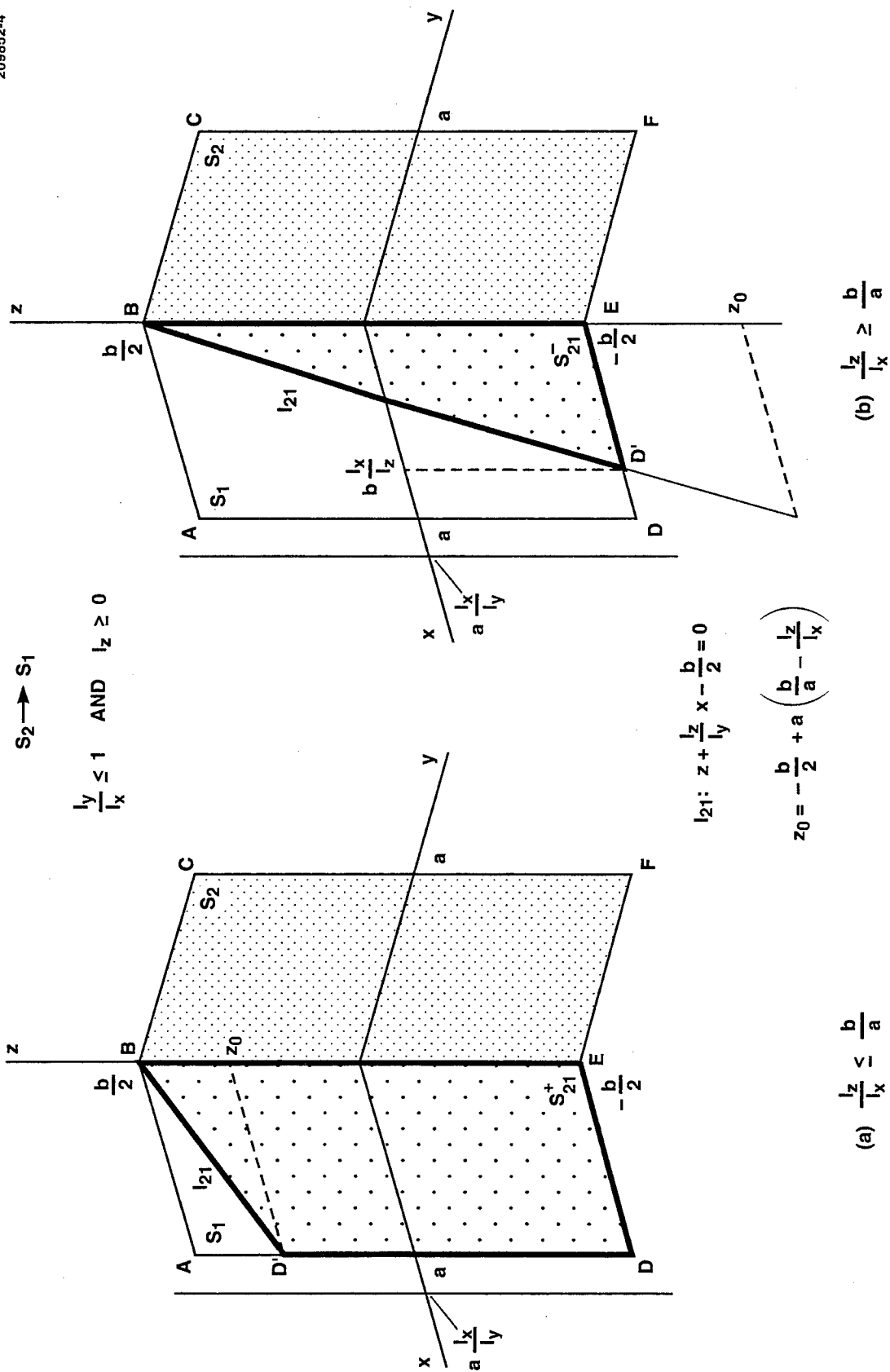


Figure 4. S_2S_1 interaction.

3.7 Simple Expressions for PS_1S_2 and PS_2S_1

Having determined the structures of the regions S_{12} and S_{21} , one can now evaluate PS_1S_2 and PS_2S_1 using Equation (52).

3.7.1 S_1S_2 Interaction

With $\hat{n}_A = \hat{y}$, $\hat{n}_B = \hat{x}$, and $\vec{r}' = (0, y, z)$, Equation (52) can be written as

$$PS_1S_2 = l_x \int_{S_{12}} e^{2ikl_z z} dS_{12}. \quad (80)$$

When $l_z/l_x \leq b/a$, the region S_{12}^+ (see Figure 3) must be used and Equation (80) becomes

$$PS_1S_2 = l_x \int_0^a \frac{l_y}{l_x} \left[\int_{-\frac{b}{2}}^{\frac{b}{2} - \frac{l_z}{l_y} y} e^{2ikl_z z} dz \right] dy. \quad (81)$$

When $l_z/l_x \geq b/a$, the region S_{12}^- (see Figure 3) must be used and Equation (80) becomes

$$PS_1S_2 = l_x \int_0^b \frac{l_y}{l_z} \left[\int_{-\frac{b}{2}}^{\frac{b}{2} - \frac{l_z}{l_y} y} e^{2ikl_z z} dz \right] dy. \quad (82)$$

3.7.2 S_2S_1 Interaction

With $\hat{n}_A = \hat{x}$, $\hat{n}_B = \hat{y}$, and $\vec{r}' = (x, 0, z)$, Equation (52) can be written as

$$PS_2S_1 = l_y \int_{S_{21}} e^{2ikl_z z} dS_{21}. \quad (83)$$

For $l_z/l_x \leq b/a$, one finds (see Figure 4)

$$PS_2S_1 = l_y \int_0^a \left[\int_{-\frac{b}{2}}^{\frac{b}{2} - \frac{l_z}{l_x} x} e^{2ikl_z z} dz \right] dx. \quad (84)$$

For $l_z/l_x \geq b/a$, one finds (see Figure 4)

$$P S_2 S_1 = l_y \int_0^{b \frac{l_x}{l_z}} \left[\int_{-\frac{b}{2}}^{\frac{b}{2} - \frac{l_z}{l_x} x} e^{2ikl_z z} dz \right] dx. \quad (85)$$

It is useful to observe that the change of variable $y = y'(l_y/l_x)$ in Equations (81) and (82) yields Equations (84) and (85), respectively. In other words, in all cases,

$$P S_1 S_2 = P S_2 S_1. \quad (86)$$

This equality can also be proved graphically. It is clear from Figures 3 and 4 that S_{12} is simply S_{21} “compressed horizontally” by a factor l_y/l_x (note the common role of z_0 in the figures). Therefore, the ratio of the integrals in Equations (80) and (83) is

$$\frac{\int_{S_{12}} e^{2ikl_z z} dS_{12}}{\int_{S_{21}} e^{2ikl_z z} dS_{21}} = \frac{l_y}{l_x}. \quad (87)$$

Equation (86) follows immediately. Note that this equality is partially a result of the inclusion of $\hat{r} \cdot \hat{n}_B$ in Equation (52).

Straightforward integration of Equations (84) and (85) yields

$$P S_1 S_2 = P S_2 S_1 = \begin{cases} \frac{abl_y}{2ikbl_z} \left[e^{ik(b-d_x)l_z} \text{sinc } k' d_x l_z - e^{-ikbl_z} \right] & \text{if } \frac{l_z}{l_x} \leq \frac{b}{a} \\ \frac{abl_y}{2ikd_x l_z} \left[\text{sinc } k' b l_z - e^{-ikbl_z} \right] & \text{if } \frac{l_z}{l_x} \geq \frac{b}{a} \end{cases} \quad (88)$$

where

$$d_x = a \frac{l_z}{l_x}. \quad (89)$$

As one would expect, the results of Equation (88) become identical when $l_z/l_x = b/a$, in which case $d_x = b$.

3.8 Simple Expressions for $\bar{Q}_{\hat{p}_t}^{S_1 S_2}$ and $\bar{Q}_{\hat{p}_t}^{S_2 S_1}$

One begins by rewriting the numerator B of the Equation (53) for $\bar{Q}_{\hat{p}_t}^{S_A S_B}$ as

$$B = [I - \hat{r}\hat{r}](\hat{n}_B \times [\hat{a}_t - 2(\hat{a}_t \cdot \hat{n}_A)\hat{n}_A]) \quad (90)$$

$$= [I - \hat{r}\hat{r}](\hat{n}_B \times \hat{a}_t) - 2(\hat{a}_t \cdot \hat{n}_A)[I - \hat{r}\hat{r}](\hat{n}_B \times \hat{n}_A) \quad (91)$$

$$= (\hat{n}_B \cdot (\hat{a}_t \times \hat{\theta}) - 2(\hat{a}_t \cdot \hat{n}_A)[\hat{\theta} \cdot (\hat{n}_B \times \hat{n}_A)])\hat{\theta} + \hat{n}_B \cdot (\hat{a}_t \times \hat{\phi})\hat{\phi} \quad (92)$$

where one has expanded the first and second $[I - \hat{r}\hat{r}](\dots)$ expressions in Equation (91) by expressions similar to Equations (63) and (62), respectively, and used the fact that $\hat{n}_B \times \hat{n}_A$ is necessarily orthogonal to $\hat{\phi}$.

1. When $\hat{p}_t = \hat{\phi}$, Equation (41) gives $\hat{a}_t = \hat{\theta}$. Using this value for \hat{a}_t and noting that $\hat{r} = \hat{\theta} \times \hat{\phi}$, Equation (92) can be reduced, and Equation (53) yields

$$\bar{Q}_{\hat{\phi}}^{S_A S_B} = -2 \frac{(\hat{\theta} \cdot \hat{n}_A)[\hat{\theta} \cdot (\hat{n}_B \times \hat{n}_A)]}{\hat{r} \cdot \hat{n}_B} \hat{\theta} + \hat{\phi}. \quad (93)$$

To further reduce the fraction above, proceed as follows. First, because $\hat{n}_B \times \hat{n}_A$ is parallel to \hat{z} , one can express this product solely in terms of its components along $\hat{\theta}$ and \hat{r} , i.e.,

$$\hat{n}_B \times \hat{n}_A = \hat{\theta}[\hat{\theta} \cdot (\hat{n}_B \times \hat{n}_A)] + \hat{r}[\hat{r} \cdot (\hat{n}_B \times \hat{n}_A)]. \quad (94)$$

Second, transform each side, say \bar{s} , of this expression by the operation $\bar{s} \cdot \hat{n}_A$, and use the fact that $(\hat{n}_B \times \hat{n}_A) \cdot \hat{n}_A = 0$. One finds

$$(\hat{\theta} \cdot \hat{n}_A)[\hat{\theta} \cdot (\hat{n}_B \times \hat{n}_A)] + (\hat{r} \cdot \hat{n}_A)[\hat{r} \cdot (\hat{n}_B \times \hat{n}_A)] = 0. \quad (95)$$

Finally, extracting from this expression the numerator appearing in Equation (93), one gets

$$\bar{Q}_{\hat{\phi}}^{S_A S_B} = 2 \frac{(\hat{r} \cdot \hat{n}_A)[\hat{r} \cdot (\hat{n}_B \times \hat{n}_A)]}{\hat{r} \cdot \hat{n}_B} \hat{\theta} + \hat{\phi}. \quad (96)$$

For the $S_1 S_2$ interaction, one has $\hat{n}_A = \hat{y}$ and $\hat{n}_B = \hat{x}$, so that Equation (96) reduces to

$$\bar{Q}_{\hat{\phi}}^{S_1 S_2} = 2 \frac{l_y}{l_x} l_z \hat{\theta} + \hat{\phi}. \quad (97)$$

For the $S_2 S_1$ interaction, one has $\hat{n}_A = \hat{x}$ and $\hat{n}_B = \hat{y}$, so that

$$\bar{Q}_{\hat{\phi}}^{S_2 S_1} = -2 \frac{l_x}{l_y} l_z \hat{\theta} + \hat{\phi}. \quad (98)$$

2. When $\hat{p}_t = \hat{\theta}$, Equation (41) gives $\hat{a}_t = -\hat{\phi}$, and then Equation (53) yields

$$\bar{Q}_{\hat{\theta}}^{S_A S_B} = \left(1 + 2 \frac{(\hat{\phi} \cdot \hat{n}_A)[\hat{\theta} \cdot (\hat{n}_B \times \hat{n}_A)]}{\hat{r} \cdot \hat{n}_B} \right) \hat{\theta}. \quad (99)$$

To further reduce the fraction above, proceed as follows. First, because $\hat{\phi}$ is orthogonal to \hat{z} , one can express $\hat{\phi}$ solely in terms of its components along \hat{n}_A and \hat{n}_B , i.e.,

$$\hat{\phi} = \hat{n}_A(\hat{\phi} \cdot \hat{n}_A) + \hat{n}_B(\hat{\phi} \cdot \hat{n}_B). \quad (100)$$

Second, transform each side, say \bar{s} , of this expression by the operation $\hat{\theta} \cdot (\hat{n}_B \times \bar{s})$. One finds

$$\hat{\theta} \cdot (\hat{n}_B \times \hat{\phi}) = (\hat{\phi} \cdot \hat{n}_A)[\hat{\theta} \cdot (\hat{n}_B \times \hat{n}_A)] \quad (101)$$

or, using the previously-used cyclic property of the mixed product,

$$(\hat{\phi} \cdot \hat{n}_A)[\hat{\theta} \cdot (\hat{n}_B \times \hat{n}_A)] = -\hat{n}_B \cdot \hat{r}. \quad (102)$$

Finally, extracting from this expression the numerator appearing in Equation (99), one gets

$$\bar{Q}_{\hat{\theta}}^{S_A S_B} = -\hat{\theta} \quad (103)$$

and, therefore,

$$\bar{Q}_{\hat{\theta}}^{S_1 S_2} = \bar{Q}_{\hat{\theta}}^{S_2 S_1} = -\hat{\theta}. \quad (104)$$

One motivation for introducing $\hat{r} \cdot \hat{n}_B$ in Equation (53) was to obtain unit-length $\bar{Q}_{\hat{\theta}}^{S_1 S_2}$ and $\bar{Q}_{\hat{\theta}}^{S_2 S_1}$ (the co-polarized components).

For horizontal transmit ($\hat{\phi}$), Equations (97) and (98) indicate that the “return” from *each* individual DB interaction has components that are both co-polarized and cross-polarized with the transmitted wave. However, when the sensor is in the plane (\hat{x}, \hat{y}) , where $l_z = 0$, the cross-polarized component vanishes. Further conclusions regarding this component will be given when the joint return for the $S_1 S_2$ and $S_2 S_1$ interactions are considered.

In the case of vertical transmit ($\hat{\theta}$), Equation (104) indicates that the “return” from *each* individual DB interaction is totally co-polarized with the transmitted wave.

3.9 Final Expression for the Backscattered Fields

Some of the results of Sections 3.6 and 3.7 were derived under the limitations of Equation (68), i.e., $l_y \leq l_x$ and $l_z \geq 0$. Simple symmetry arguments (or brute-force recalculation) show that all results can be generalized to arbitrary values of l_x , l_y , and l_z (in the allowed ranges) by defining

$$\begin{cases} l &= \max(l_x, l_y) \\ m &= \min(l_x, l_y) \\ n &= |l_z| \end{cases} \quad (105)$$

and making the substitutions

$$\begin{cases} l_x &\rightarrow l \\ l_y &\rightarrow m \\ l_z &\rightarrow n \end{cases} \quad (106)$$

throughout the preceding results.

In particular, the important dichotomy related to the sign of

$$\frac{l_z}{l_x} - \frac{b}{a} \quad (107)$$

can be generalized by considering the sign of

$$\frac{n}{l} - \frac{b}{a} \equiv \frac{|l_z|}{\max(l_x, l_y)} - \frac{b}{a}. \quad (108)$$

Because of the observed equalities in Equations (64) and (86), one can rewrite Equation (49) as

$$\bar{E}_{\hat{p}_t}(\bar{r}) = -\frac{ikE_0e^{-ikr}}{2\pi r} [(PS_1 + PS_2)\bar{Q}_{\hat{p}_t}^{S_1} + PS_1S_2(\bar{Q}_{\hat{p}_t}^{S_1S_2} + \bar{Q}_{\hat{p}_t}^{S_2S_1})] \quad (109)$$

or, in terms of SB and DB contributions,

$$\bar{E}_{\hat{p}_t}(\bar{r}) = -\frac{ikE_0e^{-ikr}}{2\pi r} (P^{SB}\bar{Q}_{\hat{p}_t}^{SB} + P^{DB}\bar{Q}_{\hat{p}_t}^{DB}) \quad (110)$$

where

$$\begin{cases} P^{SB} &= P^{S_1} + P^{S_2} \\ \bar{Q}_{\hat{p}_t}^{SB} &= \bar{Q}_{\hat{p}_t}^{S_1} \\ P^{DB} &= 2P^{S_1 S_2} \\ \bar{Q}_{\hat{p}_t}^{DB} &= 0.5(\bar{Q}_{\hat{p}_t}^{S_1 S_2} + \bar{Q}_{\hat{p}_t}^{S_2 S_1}). \end{cases} \quad (111)$$

The reason for the seemingly arbitrary factors 2 and 0.5 above is explained below.

The values of the four fundamental quantities in Equation (111) can be expressed by making the substitutions of Equation (106) in Equations (57), (60), (64), (88), (97), and (98).

One finds

$$P^{SB} = ab \operatorname{sinc} k'bn (m e^{ikal} \operatorname{sinc} k'al + l e^{ikam} \operatorname{sinc} k'am) \quad (112)$$

$$\bar{Q}_{\hat{p}_t}^{SB} = \hat{p}_t = \begin{cases} \hat{\phi} & \text{if } \hat{p}_t = \hat{\phi} \text{ (H pol)} \\ \hat{\theta} & \text{if } \hat{p}_t = \hat{\theta} \text{ (V pol)} \end{cases} \quad (113)$$

$$P^{DB} = \begin{cases} \frac{abm}{ikbn} (e^{ik(b-d_{ln})n} \operatorname{sinc} k'd_{ln}n - e^{-ikbn}) & \text{if } d_{ln} \leq b \\ \frac{abm}{ikd_{ln}n} (\operatorname{sinc} k'bn - e^{-ikbn}) & \text{if } d_{ln} \geq b \end{cases} \quad (114)$$

$$\bar{Q}_{\hat{p}_t}^{DB} = \begin{cases} -\epsilon_{lmn} \hat{\theta} + \hat{\phi} & \text{if } \hat{p}_t = \hat{\phi} \text{ (H pol)} \\ -\hat{\theta} & \text{if } \hat{p}_t = \hat{\theta} \text{ (V pol)} \end{cases} \quad (115)$$

with

$$d_{ln} = a \frac{n}{l} \quad (116)$$

and

$$\epsilon_{lmn} = \frac{l^2 - m^2}{lm} n. \quad (117)$$

One motivation for introducing the extra factors 2 and 0.5 in Equation (111) was to obtain unit-length vectors for the co-polarized components in Equation (115).

3.10 Backscattered Field for \hat{k}_t Orthogonal to Crease

In the special case where the transmitted wave travels in a direction orthogonal to the crease of the dihedral (i.e., when $n = 0$), Equations (112) to (117) can be reduced considerably. All simplifications are straightforward, except, perhaps, in the case of Equation (114). Because $d_{ln} = 0$, the first expression for P^{SB} must be used. Also, in the limit as $n \rightarrow 0$, $d_{ln}n$ approaches 0 as n^2 , whereas bn approaches 0 as n . Therefore,

$$\begin{aligned} P^{DB}(n=0) &= \lim_{n \rightarrow 0} \frac{abm}{ikbn} (e^{ikbn} - e^{-ikbn}) \\ &= 2abm \lim_{n \rightarrow 0} \text{sinc } k'bn \\ &= 2abm. \end{aligned} \tag{118}$$

Thus, for $n = 0$,

$$P^{SB}(n=0) = ab(m e^{ikal} \text{sinc } k'al + l e^{ikam} \text{sinc } k'am) \tag{119}$$

$$\bar{Q}^{SB}(n=0) = \hat{p}_t = \begin{cases} \hat{\phi} & \text{if } \hat{p}_t = \hat{\phi} \text{ (H pol)} \\ \hat{\theta} & \text{if } \hat{p}_t = \hat{\theta} \text{ (V pol)} \end{cases} \tag{120}$$

$$P^{DB}(n=0) = 2abm \tag{121}$$

$$\bar{Q}^{DB}(n=0) = \begin{cases} \hat{\phi} & \text{if } \hat{p}_t = \hat{\phi} \text{ (H pol)} \\ -\hat{\theta} & \text{if } \hat{p}_t = \hat{\theta} \text{ (V pol)} \end{cases} \tag{122}$$

with, of course,

$$l = \sqrt{1 - m^2} \text{ or } m = \sqrt{1 - l^2}. \tag{123}$$

4. DISCUSSION OF RELATION BETWEEN n/l AND b/a

This section explores the origin of the dichotomy related to the sign of the quantity $n/l - b/a$ [see Equation (108)], and analyzes the mapping of this sign on a 3-D viewing sphere.

4.1 Fundamental Observations

Consider the dihedral positioned in the (x', y', z') coordinate system as indicated in Figure 5 (note that the origin is at the bottom end E of the dihedral's crease). To simplify the discussion, consider the special form $l_z/l_x - b/a$ of the quantity $n/l - b/a$. As previously discussed, this special case arises when $l_y \leq l_x$ (i.e., $0 \leq \phi \leq \pi/4$) and $l_z \geq 0$ (i.e., $0 \leq \theta \leq \pi/2$). The conclusions reached for this special case are easily extended to the general case via symmetry.

Consider the plane AGE that contains the diagonal AE of S_1 and is perpendicular to S_1 . It is simple to show that any transmitted plane wave with wavevector $\hat{k}_t = (l_x, l_y, l_z)$ in this plane (and with $l_y \leq l_x$ and $l_z \geq 0$) satisfies the equality of interest, i.e., $l_z/l_x = b/a$. Indeed, from Figure 5, $EI = b \tan \theta$ and $EI = a / \cos \phi$, so that

$$\frac{\cot \theta}{\cos \phi} = \frac{b}{a}, \text{ i.e., } \frac{l_z}{l_x} = \frac{b}{a} \quad (124)$$

where Equation (55) was used.

If one (a) selects a particular wavevector in the previously considered plane AGE , say with direction GE (the corresponding \hat{k}_t is shown in Figure 5), (b) considers the plane GCE containing GE and perpendicular to S_2 , and (c) computes the y' coordinate of the intersection C of that plane with GH or, equivalently, the y' coordinate of F , one finds $y'_F = EI \sin \phi = a \tan \phi = al_y/l_x$. Note that the line containing CF is also the line appearing in S_2 in Figure 3.

This discussion shows that any wavevector $\hat{k}_t = (l_x, l_y, l_z)$ satisfying $l_z/l_x = b/a$ (and $l_y \leq l_x$, $l_z \geq 0$) is defined by the intersection of two planes: (a) the plane perpendicular to S_1 and containing the diagonal AE of S_1 , and (b) the plane perpendicular to S_2 and containing the diagonal CE of the rectangle $BCFE$ uniquely defined by al_y/l_x . Similar conclusions can be reached for conditions other than $l_y \leq l_x$ and $l_z \geq 0$.

The previous reasoning can be carried out elegantly via spherical trigonometry. Using the sphere shown in Figure 5 (with center E and radius a), consider some viewing direction GE . The intersection O of this line with the sphere, together with the three coordinate axes for x' , y' , and z' , define the arcs of great circle DOM , JOK , and LON , respectively (e.g., the plane through O and the x' axis defines DOM).

By applying one of Napier's rules [21, pp. 271-272] to the right spherical triangle ONJ , one finds

$$\cos \phi = \cot \theta \cot \alpha_y \quad (125)$$

which implies that $l_z/l_x = b/a$ can be satisfied only if $\tan \alpha_y = b/a$, i.e., only if the plane $JK E$ contains the diagonal AE of S_1 .

By applying a similar formula to OND , one finds

$$\sin \phi = \cot \theta \cot \alpha_x \quad (126)$$

which, given the previous constraint on α_y , gives $\tan \alpha_x = (b/a)(l_x/l_y)$, and thus $EF = al_y/l_x$.

4.2 Partitioning of the Viewing Sphere

Another advantage of the analysis on the sphere is that it provides an instant display of the partitioning of the viewing space by the boundary case $l_z/l_x = b/a$. Indeed, the boundary on the sphere of Figure 5 is the arc KOJ , restricted to $0 \leq \phi \leq \pi/4$ because of the current limitation to $l_y \leq l_x$ and $l_z \geq 0$.

A simple symmetry argument readily extends the conclusions to the general boundary case $n/l = b/a$. Figures 6(a) and 6(b) show the regions on the sphere that correspond to $n/l < b/a$ and $n/l > b/a$ for a long and a short dihedral, respectively (only for $l_z \geq 0$).

4.3 Physical Interpretation

When $l_z/l_x = b/a$, it is clear from Figures 3 and 4 that F' merges with F and D' merges with D . The resulting diagonals BF and BD are shown in Figures 7(a) and 7(b).

When $l_z/l_x = b/a$, Equation (71) reveals that the ray with direction \hat{k}_t that is reflected at A by S_1 arrives at F on S_2 . It is thus clear that the sheet of rays that is reflected by the edge AB exactly illuminates the diagonal BF , i.e., all rays incident along AB hit S_2 (along BF). This is illustrated in Figure 7(a).

As previously observed, the direction \hat{k}_t must be parallel to both the plane AEF and the plane CED . Furthermore, Equation (76) reveals that the ray with direction \hat{k}_t that is reflected at C by S_2 arrives at D on S_1 . Clearly, the sheet of rays reflected by the *partial* edge BC exactly illuminates the diagonal BD . This is illustrated in Figure 7(b).

4.4 Interpretation of Parameter d_x

A simple interpretation of the parameter d_x defined by Equation (89) can be obtained from Figure 8 (which has many elements in common with Figure 5). As shown in Section 4.1, the arc JOK (where K is on the diagonal AE) corresponds to all incidence directions \hat{k}_t related by $l_z/l_x = b/a$. This observation and the definition in Equation (89), i.e., $l_z/l_x = d_x/a$, immediately suggest a graphical construction for d_x . By first drawing the arc $JO'K'$ through the point O' corresponding to the direction \hat{k}_t of interest, and then finding the intersection A' of the lines EK' and AD , one finds that d_x is simply the length of the segment DA' . Clearly, an important value for d_x [and its equivalent d_{ln} given by Equation (116)] is b , which corresponds to $A' \equiv A$. Indeed, depending upon the relative values of d_x (or d_{ln}) and b , different expressions must be used for the DB contribution given by Equation (88) [or Equation (114)].

Figure 5. Geometry for studying sign of $l_z/l_x - b/a$.

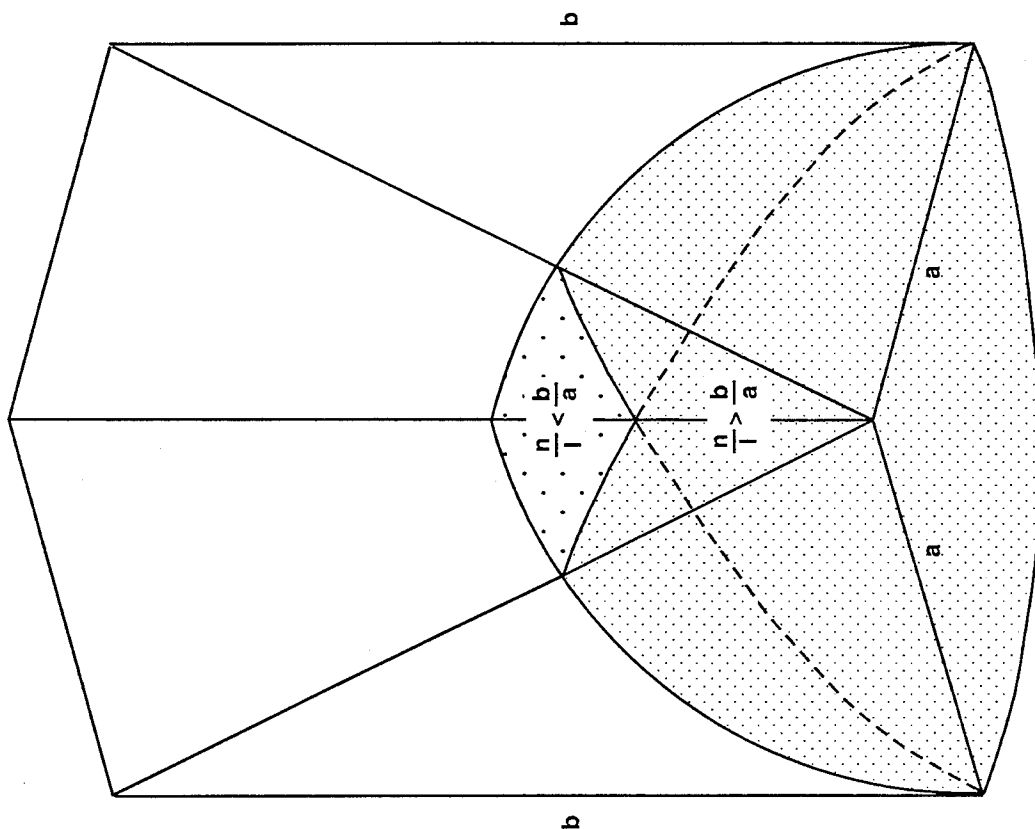
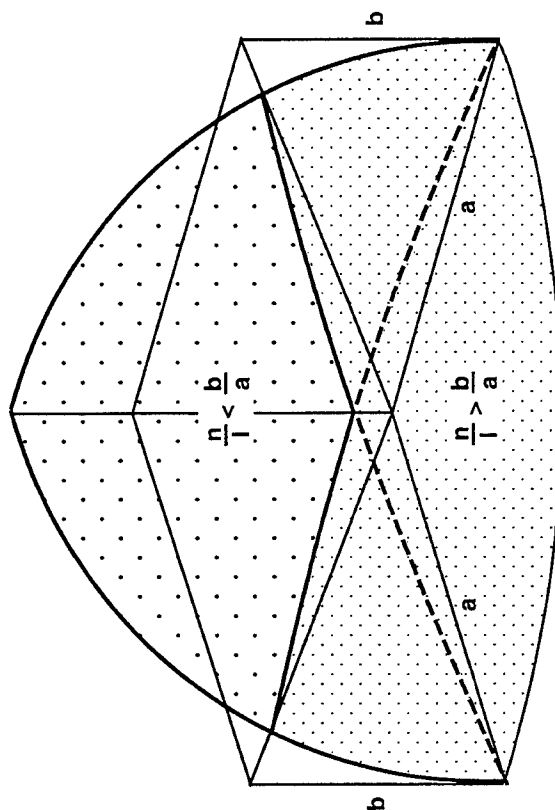
(a) LARGE $\frac{b}{a}$ (b) SMALL $\frac{b}{a}$

Figure 6. Partitioning of the viewing sphere according to the sign of $n/l - b/a$ for (a) a long dihedral (large b/a) and (b) a short dihedral (small b/a).

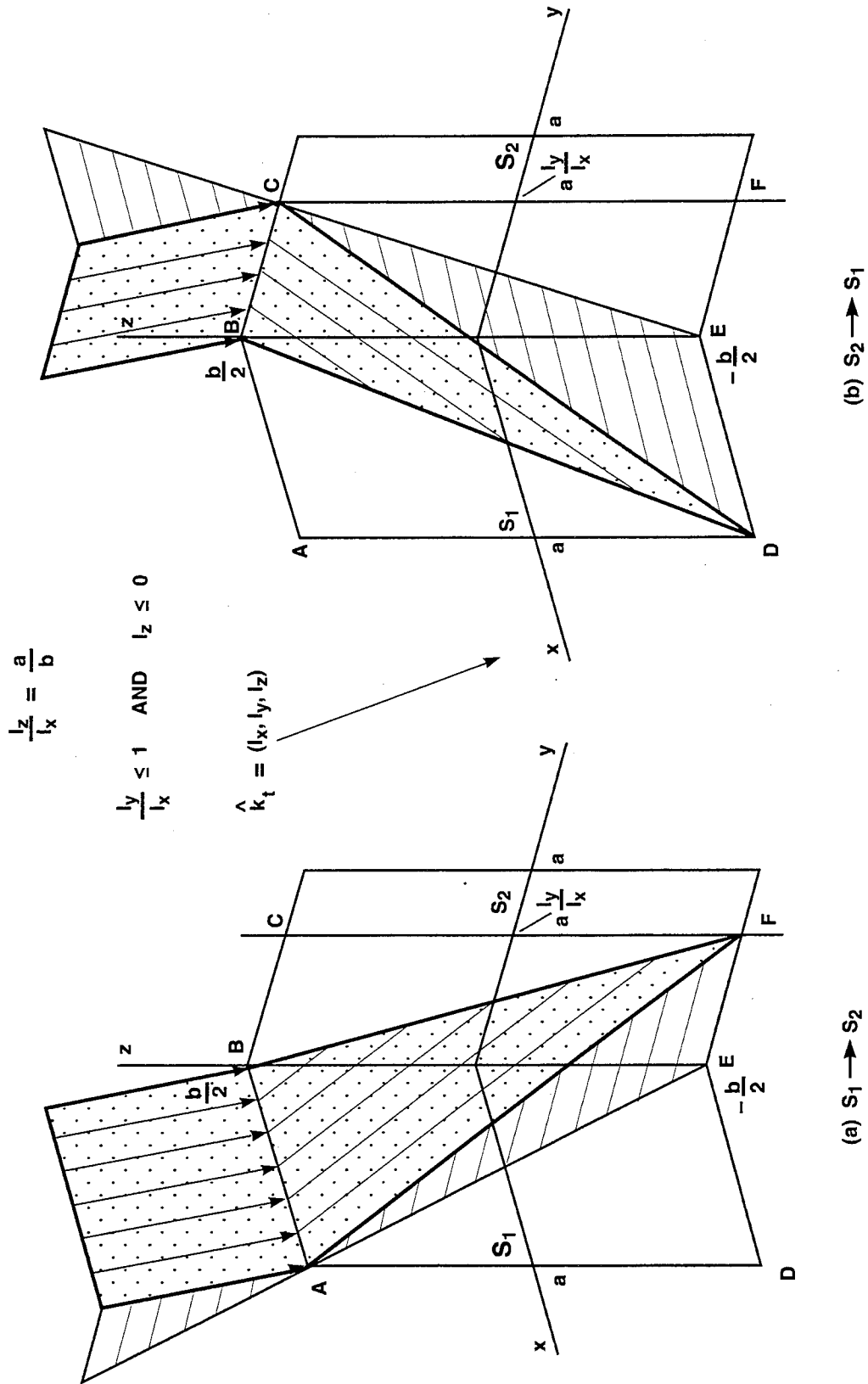


Figure 7. Interpretation of boundary case $l_z/l_x = b/a$ in terms of ray casting.

39

5. POLARIZATION SCATTERING MATRIX OF DIHEDRAL

As indicated in Section 2.4, one should first derive the complex radar cross sections $\sqrt{\sigma_{\hat{p}_r \hat{p}_t}}$ given by Equation (15). Then one can obtain the elements $S_{\hat{p}_r \hat{p}_t}$ of the scattering matrix through Equation (16). The corresponding matrices $\sqrt{\sigma}$ and S can also be related through Equation (20).

To continue keeping single-bounce (SB) and double-bounce (DB) contributions distinct, Equation (110) is rewritten as

$$\bar{E}_{\hat{p}_t}(\bar{r}) = \bar{E}_{\hat{p}_t}^{SB}(\bar{r}) + \bar{E}_{\hat{p}_t}^{DB}(\bar{r}) \quad (127)$$

with

$$\bar{E}_{\hat{p}_t}^{SB}(\bar{r}) = -\frac{ikE_0e^{-ikr}}{2\pi r} P^{SB} \bar{Q}_{\hat{p}_t}^{SB} \quad (128)$$

$$\bar{E}_{\hat{p}_t}^{DB}(\bar{r}) = -\frac{ikE_0e^{-ikr}}{2\pi r} P^{DB} \bar{Q}_{\hat{p}_t}^{DB}. \quad (129)$$

Then, Equation (15) can be rewritten as

$$\sqrt{\sigma_{\hat{p}_t \hat{p}_r}} = \sqrt{\sigma_{\hat{p}_t \hat{p}_r}^{SB}} + \sqrt{\sigma_{\hat{p}_t \hat{p}_r}^{DB}} \quad (130)$$

with

$$\sqrt{\sigma_{\hat{p}_r \hat{p}_t}^{SB}} = \lim_{r \rightarrow \infty} 2\sqrt{\pi r} \frac{\bar{E}_{\hat{p}_t}^{SB}(\bar{r}) \cdot \hat{p}_r}{E_0} e^{ikr} \quad (131)$$

$$\sqrt{\sigma_{\hat{p}_r \hat{p}_t}^{DB}} = \lim_{r \rightarrow \infty} 2\sqrt{\pi r} \frac{\bar{E}_{\hat{p}_t}^{DB}(\bar{r}) \cdot \hat{p}_r}{E_0} e^{ikr}. \quad (132)$$

5.1 Single-Bounce Complex Radar Cross-Section

The general expression for the SB C-RCS is obtained from Equations (131), (128), (112), and (113), i.e.,

$$\begin{aligned} \sqrt{\sigma_{\hat{p}_r \hat{p}_t}^{SB}} &= -\frac{ik}{\sqrt{\pi}} P^{SB} \bar{Q}_{\hat{p}_t}^{SB} \cdot \hat{p}_r \\ &= K_{\sigma}^{SB} \hat{p}_t \cdot \hat{p}_r \end{aligned} \quad (133)$$

where

$$K_{\sigma}^{SB} = -\frac{ik}{\sqrt{\pi}} P^{SB}. \quad (134)$$

Therefore

$$\sqrt{\sigma^{SB}} = K_{\sigma}^{SB} \begin{pmatrix} 1 & 0 \\ 0 & 1 \end{pmatrix}. \quad (135)$$

5.2 Double-Bounce Complex Radar Cross-Section

The general expression for the DB C-RCS is obtained from Equations (132), (129), (114), and (115), i.e.,

$$\begin{aligned} \sqrt{\sigma_{\hat{p}_r \hat{p}_t}^{DB}} &= -\frac{ik}{\sqrt{\pi}} P^{DB} \bar{Q}_{\hat{p}_t}^{DB} \cdot \hat{p}_r \\ &= K_{\sigma}^{DB} \begin{cases} -\epsilon_{lmn} \hat{\theta} \cdot \hat{p}_r + \hat{\phi} \cdot \hat{p}_r & \text{if } \hat{p}_t = \hat{\phi} \text{ (H pol)} \\ -\hat{\theta} \cdot \hat{p}_r & \text{if } \hat{p}_t = \hat{\theta} \text{ (V pol)} \end{cases} \end{aligned} \quad (136)$$

where

$$K_{\sigma}^{DB} = -\frac{ik}{\sqrt{\pi}} P^{DB}. \quad (137)$$

Therefore

$$\sqrt{\sigma^{DB}} = K_{\sigma}^{DB} \begin{pmatrix} 1 & 0 \\ -\epsilon_{lmn} & -1 \end{pmatrix} \quad (138)$$

where [see Equation (117)]

$$\epsilon_{lmn} = \frac{l^2 - m^2}{lm} n. \quad (139)$$

For an arbitrary triplet of consistent values l , m , and n (e.g., requiring that $l \geq m$), ϵ_{lmn} is generally nonzero and thus the matrix $\sqrt{\sigma^{DB}}$ is not symmetric. When $l \gg m$, one has $\epsilon_{lmn} \approx (l/m)n$, and this value can be large if n is not too small. However, these conditions correspond to large deviations of the wavevector \hat{k}_t from the principal axis of symmetry (characterized by $l = m$ and $n = 0$) and thus to viewing directions where the PO approximation would not be expected to produce accurate results. For example, it is reported in Kouyoumjian [7, p. 871] that the PO prediction for scattering from a circular plate with radius a is satisfactory only within 20 deg of normal incidence for $ka > 8.5$.

However, for orientations \hat{k}_t parallel either to the plane $l = m$ or to the plane $n = 0$, ϵ_{lmn} is precisely zero. Furthermore, ϵ_{lmn} is very small in the vicinity of the principal axis of symmetry, where PO is expected to produce accurate results. As a result, one sets ϵ_{lmn} to zero in subsequent discussions, thereby making $\sqrt{\sigma^{DB}}$ symmetric, i.e.,

$$\sqrt{\sigma^{DB}} = K_{\sigma}^{DB} \begin{pmatrix} 1 & 0 \\ 0 & -1 \end{pmatrix}. \quad (140)$$

The reason for the presence of ϵ_{lmn} in Equation (138), and thus the lack of symmetry of $\sqrt{\sigma^{DB}}$, is the failure of PO to obey the reciprocity theorem [7, 8], with the result that bistatic (double-bounce in this case) cross sections are generally erroneous.

5.3 Relative Importance of Single- and Double-Bounce Complex Radar Cross Sections

To compare the magnitude of the SB and DB C-RCS near the main axis of symmetry of the dihedral, we examine the ratio of the factors K_{σ}^{SB} and K_{σ}^{DB} [appearing in Equations (135) and (138)] in the case where $l = m = \sqrt{2}/2$ and $n = 0$. Using Equations (119) and (121), one finds

$$\rho = \left| \frac{K_{\sigma, sym}^{SB}}{K_{\sigma, sym}^{DB}} \right| = \left| \frac{P_{sym}^{SB}}{P_{sym}^{DB}} \right| = \left| \text{sinc } k'a \frac{\sqrt{2}}{2} \right| \quad (141)$$

Observe that ρ decreases towards 0 as ka increases. Furthermore, assuming $ka \geq 8$ (the requirement used in Kouyoumjian [7, p. 871] for PO to produce accurate results), one has

$$\rho \leq \left| \frac{\sin 1.5\pi}{1.5\pi} \right| = \frac{1}{1.5\pi} \approx 0.212. \quad (142)$$

Therefore, the SB C-RCS can generally be assumed to be at least 13.5 dBs below the DB C-RCS. Even though this result was derived on the main axis of symmetry, there is a tendency for the DB C-RCS to dominate whenever n is small. Keeping in mind that the results obtained through the PO approximation are valid only in the vicinity of the main symmetry axis, the contribution of the SB C-RCS can generally be ignored, and the C-RCS matrix of the dihedral is often taken as

$$\sqrt{\sigma} \approx \sqrt{\sigma^{DB}} = K_{\sigma}^{DB} \begin{pmatrix} 1 & 0 \\ 0 & -1 \end{pmatrix}. \quad (143)$$

The observation that the DB interaction is generally more important than the SB interaction was also made in Corona et al. [10].

5.4 Double-Bounce Complex Radar Cross Section on the Symmetry Axis

Setting $l = m = \sqrt{2}/2$ and $n = 0$, and using Equations (137) and (121), one finds

$$K_{\sigma, sym}^{DB} = -\frac{ik}{\sqrt{\pi}} ab\sqrt{2}. \quad (144)$$

The co-polarized DB radar cross-sections (RCSs) are thus found to be

$$\sigma_{\hat{\phi}\hat{\phi}} = \sigma_{\hat{\theta}\hat{\theta}} = \frac{2k^2 a^2 b^2}{\pi} = \frac{8\pi a^2 b^2}{\lambda^2}. \quad (145)$$

These results agree with the RCS values published, e.g. in Knott [11, Table 6-1, p. 178].

5.5 C-RCS Matrix in Circular Basis

By applying the equivalent of Equation (31) for C-RCS matrices, one can derive from the dihedral linear-basis C-RCS matrix [see Equation (143)]

$$\sqrt{\sigma_{(HV)}} = K_{\sigma}^{DB} \begin{pmatrix} 1 & 0 \\ 0 & -1 \end{pmatrix} \quad (146)$$

the dihedral circular-basis C-RCS matrix

$$\sqrt{\sigma_{(LR)}} = K_{\sigma}^{DB} \begin{pmatrix} 1 & 0 \\ 0 & 1 \end{pmatrix}. \quad (147)$$

This last expression [and *not* Equation (146)] makes the dihedral an even-bounce (circular polarization) scatterer.

APPENDIX A

TRANSFORMATION OF SCATTERING MATRIX UNDER CHANGE OF POLARIZATION BASIS

The rules governing the transformation of the scattering matrix when a change of polarization basis is performed are well-known. They are included here for completeness. This report's approach is a mix between those of Boerner et al. [22, 23] and Riegger [24].

A.1 Transformation of Basis Vectors

Consider the transformation between the polarization bases (AB) and $(A'B')$ respectively characterized by their (unit-length) basis vectors \hat{h}_A, \hat{h}_B and $\hat{h}_{A'}, \hat{h}_{B'}$, and assume that these vectors are related by Equation (24), i.e.,

$$\hat{h}_{(A'B')} = T \hat{h}_{(AB)} \quad (\text{A.1})$$

or

$$\begin{pmatrix} \hat{h}_{A'} \\ \hat{h}_{B'} \end{pmatrix} = \begin{pmatrix} T_{A'A} & T_{A'B} \\ T_{B'A} & T_{B'B} \end{pmatrix} \begin{pmatrix} \hat{h}_A \\ \hat{h}_B \end{pmatrix}. \quad (\text{A.2})$$

As one shall see shortly, T is necessarily a unitary matrix.

A.2 Transformation of Fields

Any field \bar{E} can be expressed in each of the (AB) and $(A'B')$ bases as

$$\bar{E} = E_A \hat{h}_A + E_B \hat{h}_B \quad (\text{A.3})$$

$$\bar{E} = E_{A'} \hat{h}_{A'} + E_{B'} \hat{h}_{B'}. \quad (\text{A.4})$$

By using Equation (A.2), Equation (A.4) becomes

$$\begin{aligned} \bar{E} &= E_{A'}(T_{A'A} \hat{h}_A + T_{A'B} \hat{h}_B) + E_{B'}(T_{B'A} \hat{h}_A + T_{B'B} \hat{h}_B) \\ &= (T_{A'A} E_{A'} + T_{B'A} E_{B'}) \hat{h}_A + (T_{A'B} E_{A'} + T_{B'B} E_{B'}) \hat{h}_B. \end{aligned} \quad (\text{A.5})$$

Direct comparison of Equation (A.3) and (A.5) shows that

$$\begin{pmatrix} E_A \\ E_B \end{pmatrix} = \begin{pmatrix} T_{A'A} & T_{B'A} \\ T_{A'B} & T_{B'B} \end{pmatrix} \begin{pmatrix} E_{A'} \\ E_{B'} \end{pmatrix} \quad (\text{A.6})$$

or, more compactly,

$$\bar{E}_{(AB)} = U \bar{E}_{(A'B')} \quad (\text{A.7})$$

where, in general, $\bar{E}_{(XY)}$ denotes the two-element vector containing the components of E in the (XY) basis, and

$$U = T^T. \quad (\text{A.8})$$

The fact that the total power in the (plane) wave corresponding to \bar{E} or, equivalently, the magnitude of \bar{E} , must remain constant under a change of basis leads to the requirement that U , and thus T , be unitary matrices, i.e.,

$$U^{-1} = U^{*T} \quad \text{and} \quad |\det(U)| = 1 \quad (\text{A.9})$$

$$T^{-1} = T^{*T} \quad \text{and} \quad |\det(T)| = 1. \quad (\text{A.10})$$

If (AB) is the linear basis (HV) , and $(A'B')$ an elliptical basis with arbitrary orientation ψ and arbitrary ellipticity τ , one can show that [24]

$$\bar{E}_{(HV)} = U(\psi, \tau) \bar{E}_{(A'B')} \quad (\text{A.11})$$

with

$$U(\psi, \tau) = R(\psi)H(\tau) \quad (\text{A.12})$$

where $R(\psi)$ is the rotation matrix

$$R(\psi) = \begin{pmatrix} \cos \psi & -\sin \psi \\ \sin \psi & \cos \psi \end{pmatrix} \quad (\text{A.13})$$

and $H(\tau)$ the ellipticity matrix

$$H(\tau) = \begin{pmatrix} \cos \tau & j \sin \tau \\ j \sin \tau & \cos \tau \end{pmatrix}. \quad (\text{A.14})$$

It is useful to note that $R(\psi)$ and $H(\tau)$ are unitary, with the consequence that their product, i.e., $U(\psi, \tau)$, is also unitary (as previously announced).

A.3 Transformation of Scattering Matrices

The starting point is the Equation (9) defining the scattering matrix S in the linear basis (HV) , i.e.,

$$\bar{E}_{(HV)}^r = \alpha(k, r) S_{(HV)} \bar{E}_{(HV)}^t. \quad (\text{A.15})$$

Now, as strange as it may seem, one will perform *distinct* changes of basis on the received and transmitted fields! \bar{E}^r is expressed in a basis $(A'_r B'_r)$ characterized by ψ and τ_r , and \bar{E}^t is expressed in a basis $(A'_t B'_t)$ characterized by ψ and τ_t . Therefore, using Equation (A.11), Equation (A.15) becomes

$$U(\psi, \tau_r) \bar{E}_{(A'_r B'_r)}^r = \alpha(k, r) S_{(HV)} U(\psi, \tau_t) \bar{E}_{(A'_t B'_t)}^t \quad (\text{A.16})$$

or

$$\bar{E}_{(A'_r B'_r)}^r = \alpha_{k,r} U^{-1}(\psi, \tau_r) S_{(HV)} U(\psi, \tau_t) \bar{E}_{(A'_t B'_t)}^t. \quad (\text{A.17})$$

By generalizing Equation (A.15) to the case of distinct receive and transmit bases, one can write

$$\bar{E}_{(A'_r B'_r)}^r = \alpha(k, r) S_{(A'_r B'_r, A'_t B'_t)} \bar{E}_{(A'_t B'_t)}^t. \quad (\text{A.18})$$

Comparing Equations (A.17) and (A.18), one gets

$$S_{(A'_r B'_r, A'_t B'_t)} = U^{-1}(\psi, \tau_r) S_{(HV)} U(\psi, \tau_t). \quad (\text{A.19})$$

When $\tau_r = \tau_t = \tau$, Equation (A.19) describes a *true change of basis*, i.e.,

$$S_{(A'B')} = U^{-1} S_{(HV)} U = U^{*T} S_{(HV)} U \quad (\text{A.20})$$

where $(A'B') = (A'_t B'_t) = (A'_r B'_r)$ and $U = U(\psi, \tau)$. However, this is *not* the formula to use for transforming S .

The correct transformation is obtained by using $\tau_r = -\tau_t = -\tau$, in which case Equation (A.19) describes a *pseudo change of basis*, i.e.,

$$S_{(A'_r B'_r, A'_t B'_t)} = U^{-1}(\psi, -\tau) S_{(HV)} U(\psi, \tau). \quad (\text{A.21})$$

It is easy to see that $U^{-1}(\psi, -\tau) = U^T(\psi, \tau)$, so that

$$S_{(A'B')} = U^T S_{(HV)} U \quad (\text{A.22})$$

where it is understood that $U = U(\psi, \tau)$ corresponds to the $(A_t B_t)$ basis and that the subscript $(A'B')$ corresponds to the basis the transmitted field is transformed into. The transformation applied to the received field need not be known in order to use Equation (A.22), but it is easy to see that

$$U(\psi, -\tau) = (U^T)^{-1} = U^*. \quad (\text{A.23})$$

Even though Equation (A.22) is the classical formula for transforming a scattering matrix, it is, once again, important to understand that this formula does *not* describe a true change of basis [24, p. 21].

Equation (A.22) can easily be generalized to handle transformations between arbitrary bases, say (AB) and $(A'B')$. Using Equation (A.22), one has

$$\begin{cases} S_{(A_1 B_1)} &= U_1^T S_{(HV)} U_1 \\ S_{(A_2 B_2)} &= U_2^T S_{(HV)} U_2. \end{cases} \quad (\text{A.24})$$

It follows that

$$(U_1^T)^{-1} S_{(A_1 B_1)} U_1^{-1} = (U_2^T)^{-1} S_{(A_2 B_2)} U_2^{-1} \quad (\text{A.25})$$

and thus

$$S_{(A_2 B_2)} = (U_1^{-1} U_2)^T S_{(A_1 B_1)} (U_1^{-1} U_2). \quad (\text{A.26})$$

Furthermore, Equation (A.7) gives

$$\begin{cases} \bar{E}_{(HV)} &= U_1 \bar{E}_{(A_1 B_1)} \\ \bar{E}_{(HV)} &= U_2 \bar{E}_{(A_2 B_2)} \end{cases} \quad (\text{A.27})$$

so that

$$\bar{E}_{(A_1 B_1)} = U_1^{-1} U_2 \bar{E}_{(A_2 B_2)}. \quad (\text{A.28})$$

Therefore, it is clear from Equations (A.26) and (A.28) that if

$$\bar{E}_{(AB)} = U \bar{E}_{(A' B')} \quad (\text{A.29})$$

then

$$S_{(A' B')} = U^T S_{(AB)} U \quad (\text{A.30})$$

which is the desired generalization of Equation (A.22). Furthermore, note that Equation (A.29) is identical to Equation (A.7) so that $U = T^T$ [see Equation (A.8)] where T is the matrix relating the basis vectors of the bases (AB) and $(A' B')$.

It should be observed that Equation (A.30) guarantees the conservation of the voltage (see [23, p. 211])

$$V = \bar{E}_{(AB)}^T S_{(AB)} \bar{E}_{(AB)} \quad (\text{A.31})$$

under a pseudo change of basis. Indeed, using Equations (A.29) and (A.30), Equation (A.31) becomes

$$\begin{aligned} V &= \bar{E}_{(A'B')}^T U^T S_{(AB)} U \bar{E}_{(A'B')} \\ &= \bar{E}_{(A'B')}^T S_{(A'B')} \bar{E}_{(A'B')}. \end{aligned} \quad (\text{A.32})$$

APPENDIX B

ALTERNATE FORMULAS FOR THE TOTAL BACKSCATTERED FIELD

Here, one uses Equations (110), (112), (113), (114), and (115) to derive a set of new expressions for the total backscattered field $\bar{E}_{\hat{p}_i}$. These expressions are written in a form that is as close as possible to results derived by Corona et al. [10]. The algebraic manipulations required to achieve this goal have the effect of mixing the SB and DB contributions (which may not always be desirable).

When $n/l \leq b/a$, one has

$$\begin{aligned}
 \bar{E}_{\hat{\phi}}(\bar{r}) = & \\
 & -\frac{ikE_0e^{-ikr}}{2\pi r}ab \\
 & [\text{sinc } k'bn(m e^{ikal} \text{sinc } k'al + l e^{ikam} \text{sinc } k'am + 2m) \\
 & -\frac{m}{ikbn}e^{ikbn}(1 - e^{-ikd_{ln}n} \text{sinc } k'd_{ln}n)]\hat{\phi} \\
 & +\frac{ikE_0e^{-ikr}}{2\pi r}ab\frac{l^2 - m^2}{l}n \\
 & [2 \text{sinc } k'bn - \frac{1}{ikbn}e^{ikbn}(1 - e^{-ikd_{ln}n} \text{sinc } k'd_{ln}n)]\hat{\theta}
 \end{aligned} \tag{B.1}$$

$$\begin{aligned}
 \bar{E}_{\hat{\theta}}(\bar{r}) = & \\
 & -\frac{ikE_0e^{-ikr}}{2\pi r}ab \\
 & [\text{sinc } k'bn(m e^{ikal} \text{sinc } k'al + l e^{ikam} \text{sinc } k'am - 2m) \\
 & +\frac{m}{ikbn}e^{ikbn}(1 - e^{-ikd_{ln}n} \text{sinc } k'd_{ln}n)]\hat{\theta}.
 \end{aligned} \tag{B.2}$$

When $n/l \geq b/a$, one has

$$\begin{aligned}
\bar{E}_{\hat{\phi}}(\bar{r}) = & -\frac{ikE_0e^{-ikr}}{2\pi r}ab \\
& [\text{sinc } k'bn(m e^{ikal} \text{sinc } k'al + l e^{ikam} \text{sinc } k'am + \frac{m}{ikd_{ln}n}) \\
& -\frac{m}{ikd_{ln}n}e^{-ikbn}]\hat{\phi} \\
& +\frac{ikE_0e^{-ikr}}{2\pi r}ab\frac{l^2-m^2}{l}n \\
& [\frac{1}{ikd_{ln}n}(\text{sinc } k'bn - e^{-ikbn})]\hat{\theta}
\end{aligned} \tag{B.3}$$

$$\begin{aligned}
\bar{E}_{\hat{\theta}}(\bar{r}) = & -\frac{ikE_0e^{-ikr}}{2\pi r}ab \\
& [\text{sinc } k'bn(m e^{ikal} \text{sinc } k'al + l e^{ikam} \text{sinc } k'am - \frac{m}{ikd_{ln}n}) \\
& +\frac{m}{ikd_{ln}n}e^{-ikbn}]\hat{\theta}.
\end{aligned} \tag{B.4}$$

The Equations (B.1) and (B.2) become very similar, but not identical, to the Equations (22) and (21) of Corona et al. [10] when l , m , and n are expressed in terms of ϕ and θ through Equations (105) and (55). The differences are limited to the signs of some of the terms in the equations and the signs of the exponents in some of the complex exponentials. Of course, these sign differences are important. The author of this report has not been able to explain these differences.

The dichotomy related to the sign of $n/l - b/a$ is overlooked in Corona et al. [10]. Retrospectively, the analysis in [10] corresponds to the case $n/l \leq b/a$. Thus, the equivalents of Equations (B.3) and (B.4) do not appear in [13].

REFERENCES

1. A. Kozma, A.D. Nichols, R.F. Rawson, S.J. Shackman, C.W. Haney, and J.J. Shanne, "Multifrequency-polarimetric SAR for remote sensing," in *Proc. IGARSS '86 Symposium, ESA SP-254*, (1986), pp. 715-720, Zürich, Switzerland.
2. H. A. Zebker and J.J. van Zyl, "Imaging radar polarimetry: A review," in *Proc. of the IEEE*, 79(11), (1991), pp. 1583-1606.
3. J.C. Henry, T.J. Murphy, and K.M. Carusone, "The Lincoln Laboratory millimeter-wave synthetic aperture radar (SAR) imaging system," in *Synthetic Aperture Radar*, in *Proc. of SPIE, Vol. 1630*, eds. R.D. McCoy and M.E. Tanenhaus, Los Angeles, CA, (1992), pp. 35-52.
4. S. Zabele, S. Bachinsky, B. Myers, and A. Stiehl, "Signature prediction user's manual (version 7.1)," The Analytical Sciences Corporation (TASC), Reading, MA, Technical Report, TR 5345-1, (1990).
5. J.R. Huynen. *Phenomenological Theory of Radar Targets*, Rotterdam, Holland: Drukkerij Bronder-Offset N.V., (1970), Ph.D. Dissertation.
6. W.L. Cameron and L.K. Leung, "Feature motivated polarization scattering matrix decomposition," in *Proc. of the IEEE International Conference on Radar*, (1990), pp. 549-557.
7. R.G. Kouyoumjian, "Asymptotic high-frequency methods," in *Proc. of the IEEE*, 53(8) (1965), pp. 864-876.
8. D.J. Blejer, Private Communication.
9. D.J. Blejer, Private Communication.
10. P. Corona, G. Ferrara, and C. Gennarelli, "A simple and practical reference target for RCS measurements," *Alta Frequenza*, 54(4), 261-267, (1985).
11. E.F. Knott, "RCS reduction of dihedral corners," *IEEE Transactions on Antennas and Propagation*, AT-25(3), 406-409, (1977).
12. T.G. Griesser and C.A. Balanis, "Backscatter analysis of dihedral corner reflectors using physical optics and the physical theory of diffraction," *IEEE Transactions on Antennas and Propagation*, 35(10), 1137-1147, (1987).
13. P. Corona, G. Ferrara, and C. Gennarelli, "Backscattering by loaded and unloaded dihedral corners," *IEEE Transactions on Antennas and Propagation*, 35(10), 1148-1153, (1987).
14. W.C. Anderson, "Consequences of nonorthogonality on the scattering properties of dihedral reflectors," *IEEE Transactions on Antennas and Propagation*, 35(10), 1154-1159, (1987).

REFERENCES

(Continued)

15. R.G. Atkins and R.T. Shin, "A physical optics technique for prediction of multiple reflections from polygonal plate structures," *Journal of Electromagnetic Waves and Applications*, 2(8), 687-712, (1988).
16. J.A. Kong, "*Electromagnetic Wave Theory*," Second Edition, New York, NY: John Wiley & Sons, Inc., (1990).
17. G. Sinclair, "The transmission and reception of elliptically polarized waves," in *Proc. IRE*, 38 (1950), pp. 148-151.
18. E.M. Kennaugh, "Effects of the type of polarization on echo characteristics," Antenna Laboratory, Ohio State University, Technical Report 389-9, (1951).
19. H.C. Van de Hulst, *Light Scattering by Small Particles*, New York, NY: Dover, (1981).
20. A.K. Bhattacharyya and D.L. Sengupta, *Radar Cross Section Analysis & Control*, Boston, MA: Artech House, (1991).
21. W. Gellert, H. Küstner, M. Hellwich, and H. Kästner, *The VNR Concise Encyclopedia of Mathematics*, New York, NY: Van Nostrand Reinhold Company, (1977).
22. W-M. Boerner, W-L. Yan, A-Q. Xi, and Y. Yamaguchi, "On the basic principles of radar polarimetry: the target characteristic polarization state theory of Kennaugh, Huynen's polarization fork concept, and its extension to the partially polarized case," in *Proc. of the IEEE*, 79(10), (1991), pp. 1538-1550.
23. W-M. Boerner, W-L. Yan, A-Q. Xi, and Y. Yamaguchi, "Basic concepts of radar polarimetry," eds. W-M. Boerner et al., *Direct and Inverse Methods in Radar Polarimetry (Part 1)*, Dordrecht: Kluwer Academic Publishers, (1992), pp. 155-245.
24. S. Riegger and W. Wiesbeck, "Wide-band polarimetric signatures as a basis for target classification," ed. W. R. Stone, *Radar Cross Sections of Complex Objects*, New York, NY: IEEE Press, New York, NY, (1990), pp. 17-29.

REPORT DOCUMENTATION PAGE

Form Approved
OMB No. 0704-0188

Public reporting burden for this collection of information is estimated to average 1 hour per response, including the time for reviewing instructions, searching existing data sources, gathering and maintaining the data needed, and completing and reviewing the collection of information. Send comments regarding this burden estimate or any other aspect of this collection of information, including suggestions for reducing this burden, to Washington Headquarters Services, Directorate for Information Operations and Reports, 1215 Jefferson Davis Highway, Suite 1204, Arlington, VA 22202-4302, and to the Office of Management and Budget, Paperwork Reduction Project (0704-0188), Washington, DC 20503.

1. AGENCY USE ONLY (Leave blank)		2. REPORT DATE 7 February 1995		3. REPORT TYPE AND DATES COVERED Technical Report	
4. TITLE AND SUBTITLE Physical Optics Polarization Scattering Matrix for a Right-Angle Dihedral				5. FUNDING NUMBERS C — F19628-95-C-0002 PR — 222 PE — 63250F	
6. AUTHOR(S) Jacques G. Verly					
7. PERFORMING ORGANIZATION NAME(S) AND ADDRESS(ES) Lincoln Laboratory, MIT P.O. Box 9108 Lexington, MA 02173-9108				8. PERFORMING ORGANIZATION REPORT NUMBER TR-1008	
9. SPONSORING/MONITORING AGENCY NAME(S) AND ADDRESS(ES) Electronic Systems Center Hanscom AFB Bedford, MA 01731-5000				10. SPONSORING/MONITORING AGENCY REPORT NUMBER ESC-TR-94-092	
11. SUPPLEMENTARY NOTES None					
12a. DISTRIBUTION/AVAILABILITY STATEMENT Approved for public release; distribution is unlimited.				12b. DISTRIBUTION CODE	
13. ABSTRACT (Maximum 200 words) Using the geometrical optics (GO) and physical optics (PO) approximations, a correct, complete, ready-to-use formula is derived from the backscatter (monostatic) polarization scattering matrix (PSM) of the perfectly conducting right dihedral at arbitrary incidence angle. The absence of such a result from the literature is surprising given that the dihedral's PSM is needed in many applications, such as in the calibration of polarimetric radars, including synthetic aperture radars (SAR), in the generation of simulated polarimetric radar imagery, and in automatic target recognition (ATR). Because the new results provided are important to many researchers who may not be experts in electromagnetic theory (as is often the case for the computer-vision researchers working on ATR), the report is relatively self-contained and takes the reader from the definitions of PSMs and complex radar cross-sections, through the mathematical formulation of Huygen's Principle, the combined use of GO and PO, and changes of polarization bases, to the derivation, discussion, and simplification of the dihedral's PSM.					
14. SUBJECT TERMS dihedral polarization optics computer vision corner reflector polarization scattering matrix polarimetry physical optics automatic target recognition				15. NUMBER OF PAGES 66	
				16. PRICE CODE	
17. SECURITY CLASSIFICATION OF REPORT Unclassified	18. SECURITY CLASSIFICATION OF THIS PAGE Unclassified	19. SECURITY CLASSIFICATION OF ABSTRACT Unclassified	20. LIMITATION OF ABSTRACT Same as Report		